Journal of Danish Archaeology vol. 9, 1990, pp 64–102

A Metallurgical Study of 12 Prehistoric Bronze Objects from Denmark

by VAGN F. BUCHWALD and PETER LEISNER

INTRODUCTION

Scandinavian museums are rich in bronze objects. Only an insignificant fraction of them have been examined with a view to studying their metallurgy and structure. While prehistoric copper or bronze finds from Sweden (e.g. Oldeberg 1974), Britain (e.g. Coghlan 1967, Northover 1982, Parker 1982), Wales (e.g. Savory 1980), Switzerland (e.g. Rychner 1984), Italy (e.g. Matteoli and Storti 1982), and Sardinia (e.g. Tylecote et al. 1983) have been thoroughly discussed, much remains to be done on bronzes from Denmark.

The present paper is the first of a small series, in which ancient Danish bronze objects will be described from a metallurgical, a chemical, and a technological point of view. Since our method requires the removal of a substantial sample, the available objects are limited to common tools and weapons, while more valuable museum pieces will normally be out of reach.

Ten of the objects presented here have previously been analyzed by classical spectrographic methods (Junghans et al. 1960, 1968), and we have compared our new data with the spectrographic data. Generally there is very good agreement.

It has not been a primary goal of this study to map and discuss the trace elements in bronze. Rather, we have concentrated on the major elements which confer strength, coherence, castability, and corrosion resistance to the objects, in short the technological factors. While we do report some trace element data, our sample of only 12 objects is too small for any far-reaching conclusions to be drawn with respect to the origin of the bronze and the raw materials.

THE SELECTION OF SAMPLES

The present sample consists of ten axes from the Neolithic or earliest part of the Bronze Age and two lurs from the Late Bronze Age. All of them were found in Denmark, but a couple of the bronze axes are not further provenanced. Information about datings has been kindly communicated to us by Dr. D. Liversage, National Museum, who has also been helpful in other ways. The specimens have not been subjected to major conservation, so the analytical and structural data should provide a true picture of the ancient technology and the subsequent long exposure to soil corrosion.

SAMPLE PREPARATION – REQUIREMENTS AND LIMITATIONS

Wedge shaped pieces were removed from the cutting-edge and the side of each axe using a fine-toothed jeweller's saw, so that these different parts could be compared with respect to composition and technology. A trial made by the National Museum's conservation laboratory showed that the axes could if wished be restored so well that the cuts were virtually invisible.

The lurs were sampled by hacksawing or breaking small pieces from larger fragments.

The weight of the samples removed and embedded was usually less than 3 g, and the loss by hack-sawing less than 0.3 g. Generally, 60–150 mm^2 cut and polished surface was available for the study of each sample, sufficient for revealing both macrostructure, including segregation and porosity, and microstructure.

After cutting, the sample was set in cold-curing resin (Struers Epofix) in a small vacuum box. For this operation a thick-walled glass-desiccator with water-jet pumping was found to be sufficient. The vacuum impregnation served to fill pores and crevices, and to bind any loose particles that might otherwise become loose under the grinding and polishing operations and thereby scratch the finished surface.

Most samples were after mounting ground and polished on a horizontal wheel revolving at about 300 rpm,

using carborundum of increasing fineness from 80 to 1000 mesh in three or four steps. During grinding, a copious stream of water served to remove the dust and cool the sample. For the smaller samples the coarser grits were usually omitted and grinding was limited to wet emery paper, grade 1000.

Polishing was carried out on horizontal discs with cloths impregnated with diamonds (Struers DP-9 and DP-U2). The grain sizes were 3 and 1 μm.

The samples as polished were examined for defects, pores, slag distribution, and corrosion products. Afterwards, the samples were etched, either with $Cu(NH)_4Cl_2$ or with $FeCl_3$, and photomicrographs were taken and microhardness tests performed. Finally, the samples were repolished, carbon-coated, and analyzed.

CHEMICAL COMPOSITION, X-RAY ANALYSIS

The structural examination of the etched samples formed the basis of the subsequent bulk chemical analysis, which was carried out as an X-ray microprobe examination. Sufficient area was scanned so that a true picture of the bulk composition was reached, including inclusions and segregation (coring) effects. After a number of introductory analyses of various standards it was decided to scan whenever possible areas of 0.4 × 0.25 mm^2 in order to include a sufficient number of dendrite arms, coring, and sulphide inclusions.

The analytical equipment was a scanning electron microscope with an energy-dispersive X-ray analytical detector attached (Philips SEM 505 with EDAX 9100). The method is based upon element-specific X-ray fluorescence (Goldstein et al. 1984). When a plane-polished sample is exposed to a beam of high-voltage electrons, some electrons of the sample will be excited and leave their normal shells and be replaced immediately by other electrons from higher energy levels, thereby emitting X-rays characteristic of their loss of potential energy. The energy (eV) of the emitted X-rays is analyzed in a detector; the location of the channels identify the element, the intensity of the channels the concentration of the element. The equipment was operated at 30 kV, tilt 30°, take off 38.7°, and background generally at 2.8 and 14.0 eV.

The X-ray microanalytical technique was used to study the average chemical composition of a volume by scanning a typical polished area of 0.4 × 0.25 mm^2. Since the penetration of the electron beam is about 1 μm, the volume scanned is about 10^{-4} mm^3, corresponding to only about 8×10^{-7} g. Even this minute amount appears to give a true picture of the composition to better than ±5%.

In addition, the technique was applied for identification of inclusions as small as 5 μm across. The electron beam can be focused for spot analysis of, for instance, sulphide inclusions. Further possibilities are photographing the area analyzed by scanning electron microscope (SEM), e.g. fig. 2, and mapping the element distribution by photographing the X-ray image of characteristic scanned areas, e.g. figs. 56–62.

Spectral lines from two different elements may overlap making it difficult to quantify some pairs of elements correctly. It requires, for example, caution when the sample contains both lead and sulphur, or tin and antimony, or arsenic and lead. Also, it is necessary to correct for fluorescence and absorption effects, but these problems have been well studied and the machine programs (NBS/EDAX FRAME C) usually handle them satisfactorily.

We present quantitative data for the following nine elements: tin, sulphur, iron, nickel, zinc, arsenic, silver, antimony, and lead. The limit of detection with our method is 0.07–0.1 wt.%.

Sulphur occurs as the copper sulphide, Cu_2S, which may be identified on polished sections and measured by planimetry. For example, a specimen which exhibits 1.5% by volume Cu_2S, contains about $32 \times 1.5/(32+2 \times 63.5)$ wt.% S, or 0.3 wt.% S. The precision is estimated to be ±10%. The composition of the sulphides may be verified by EDAX. Sometimes small amounts of iron substitute for copper in the sulphides. Sulphur may also be determined by EDAX. However, if lead is also present the S value becomes erroneously high, and the only reliable method is planimetry.

Iron, nickel, cobalt, zinc, and *silver* were found to be present in small amounts only. They were determined by EDAX and presented no analytical problems on either polished or etched sections on the level of ±10%. Iron turns out to be essentially concentrated in the copper sulphide inclusions. Nickel is partitioned between the α- and the δ-phases, and concentrated by a factor of more than 3 in the δ-phase.

The quantitative determination by EDAX of *lead* in bronze surprisingly turned out to be a problem, even when no sulphur was present. Lead occurs as discrete, interdendritic blebs, typically 2–20 μm across, which are rather uniformly distributed through the alloy. On routine polishing, the ductile copper phase is smeared over

the soft lead pockets, thereby erroneously increasing the Cu-signal and decreasing the Pb-signal. It was found that the best procedure for a good lead analysis was to polish and etch, then polish and etch again. By these repeated operations the smeared copper was dissolved and the lead pockets exposed to their true extent. The lead amount was, in addition, estimated by planimetry under the optical microscope.

Tin, on the other hand, was determined on repolished sections, since it was found that it became enhanced upon etching, probably because copper was selectively dissolved. Tin occurs in solid solution in the copper phase, and at higher concentrations forms the intermetallic compound $Cu_{31}Sn_8$, the so-called δ-phase.

Antimony is determined by EDAX on polished sections. Antimony segregates with tin in the cast alloy but will be homogeneously distributed after annealing. Since tin and antimony have overlapping lines we found it necessary to introduce correction factors for the two elements, based upon the examination of polished standard-alloys.

Arsenic may be determined by EDAX on polished sections when lead is not present in the alloy. If lead is present, and this may be verified on microscopical examination, the arsenic and the lead values become unreliable, because the two lines (As K_α 10.530 eV and Pb L_α 10.550 eV) cannot be separated quantitatively by the Philips machinery and program. Lead is then determined by planimetry (see above), and the lower limit of arsenic is quoted. In some cases it was noted that arsenic was difficult to reproduce, perhaps because of segregation effects. On the whole, arsenic turned out to be the least reliable in our analytical set.

Copper has been found by subtraction from 100%.

All analytical results are the average of at least three analyses, performed on three different, uncorroded areas.

THE HARDNESS TEST

A technologically important characteristic of metal alloys is the hardness. The Vickers hardness number is in the order of 35–45 for unalloyed, annealed copper, but increases to above 300 for cold-worked arsenical and tin bronzes. A great deal is known about hardness and its variation, and it is safe to say that a hardness determination combined with a structural examination and a chemical analysis will usually fully characterize any sample.

The Vickers hardness test is an indentation method, where a small diamond in the shape of a pyramid is pressed into the surface by a standard load. The hardness is a measure of the resistance to indentation as measured by the diameter of the impression. The hardness number HV is defined as the load of the indenter (kg) divided by the projected area of contact between the pyramid and the metal (mm^2). In the present study the load was chosen as 5 kg in order to produce a sizable indentation, that integrated a number of grains and/or dendrite arms. Sometimes on porous or corroded materials it was difficult to arrive at reproducible hardness values. Porous objects give too low a hardness value. The test machine is a Universal Test Apparatus (Otto Wolpert Diatestor), equally well suited for Vickers, Brinell, and Rockwell tests in the range 1–250 kg.

For the detailed study of inclusions, coring etc., a microhardness test with a load of 100 g was carried out using a special test machine, the Leitz Durimet (Blau & Lawn 1985). The microhardness testing is slightly slower than the macrohardness testing and it requires a perfect, vibration-free support. With the microhardness method the gradual hardness increase from the massive interior of an axe to the work-hardened cutting-edge could easily be determined.

The hardness of all axes has been mapped in both the cutting-edge (A) and the bulk (B), see e.g. fig. 22. The values obtained at 5 kg load (underlined) are considered the most representative, and they may be directly compared to the experimental data of the curves, figs. 1, 18–20, and 87. The other values, obtained at 100 g load, are considered supplementary; they are especially important on porous or corroded objects.

A COMPARATIVE STUDY OF SYNTHETIC ALLOYS

In order to study the properties of copper alloys within the range encountered in ancient bronze objects, a number of alloys were prepared and studied. The alloys were prepared from analytical grades of tin, antimony, bismuth, sulphur (added as CuS), iron, zinc, and silver. The copper itself was cable copper (electrolyte copper with 99.95% Cu), while arsenic was added as a copper-arsenic alloy with 10.3% As. The samples were produced without phosphorus additions, since phosphorus is not present in ancient alloys.

Samples of 20 g were cast in graphite crucibles covered with graphite lids. The solidification from the casting

temperature (1100–1125 °C) took place by free cooling in air, resulting in solidification within a few minutes and formation of dendrites with an arm spacing of typically 30–50 μm, figs. 2–3.

Copper-tin

According to the equilibrium diagram (Metals Handbook 1973) copper can dissolve up to 15.8% tin. The homoge-

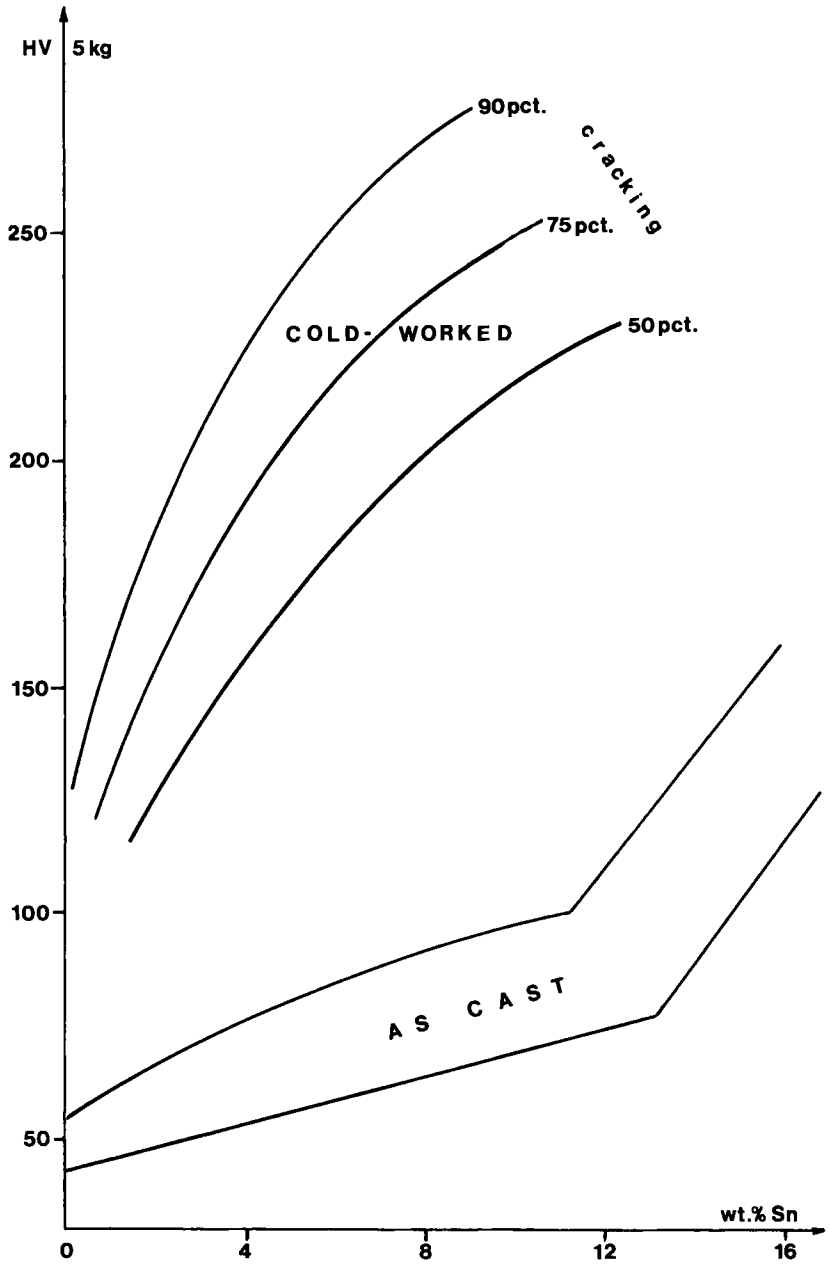

Fig. 1. Vickers hardness (5 kg load) of Cu-Sn alloys (no P-additions). Cast objects are found within the basal band. Small, rapidly cooled objects lie near the upper limit, large, slowly cooled objects near the lower limit. Fully annealed (or recrystallized) alloys are also near the lower limit. Cold-working leads to progressively harder alloys. Excessive cold-work makes the objects crack.

neous α-phase will with increasing amounts of tin in solid solution increase in hardness from about 40 to about 80. When the homogeneous phases are cold-worked, by hammering, rolling, or bending for example, the hardness increases substantially. For an evaluation of the degree of cold-work the approximate expression

$$D = (t_o - t)/t_o$$

may be used. t_o is the specimen thickness at start, and t is the thickness after cold-work. D is the degree of reduction (cold-work) in percent – it can approach but never reach 100%. It is difficult in practical work to exceed reductions of 80% in copper alloys of our interest. The more δ-phase the less reduction in cold-working is achieved before the material splits open.

In fig. 1 the hardness of copper-tin alloys is shown. Cast alloys are found within the lower band. The band is rather wide, because hardness is also a function of grain size, fine-grained alloys being harder than coarse-grained. Thus, small objects being cast in stone – or clay moulds solidify in a fine-grained structure and will tend to have hardnesses along the upper limit, while kilogram-sized objects cast in sand will be coarse-grained and have hardnesses near the lower limit. Fully annealed copper-alloys, regardless of their former treatment, will also lie near the lower limit.

Up to 15% Sn, or in normal practice to about 13% Sn, the annealed Cu-Sn alloys are homogeneous, one-phased α-alloys. With more tin increasing amounts of the hard δ-phase, $Cu_{31}Sn_8$, will occur, which will considerably increase the hardness of the alloys. In unequilibrated cast alloys the δ-phase is very common, even down to about 5 wt.% Sn. This is one reason for cast alloys having a slightly higher hardness than annealed ones.

As mentioned above, cold-working increases the hardness. In fig. 1 three curves show the progressive hardening as samples are reduced 50, 75, and 90% by cold-working. Cold-working may increase the hardness by a factor of up to 3.5 relative to the hardness of the annealed state. On recrystallization and annealing the high hardness will revert to the low values shown in the basal band. No doubt, the ancient metal worker was well aware of these facts and was able to work and anneal repeatedly until what he was making had reached the desired shape and strength. The internal structure of the metal changes very much during this work. A selection of typical structural steps are shown in figs. 3–9.

The hardness of a metal is a property which is rather easily measured. It is interesting to note that the mechanical strength is closely related to the hardness. The ultimate tensile strength, measured in N/mm^2, is about 3 times the hardness measured on the Vickers scale.

For further information on the hardness and strength of copper alloys the reader may consult, e.g., Metals Handbook, Wilkins & Bunn (1943), Dies (1967), and Hanson & Pell-Walpole (1951).

Copper-tin-sulphur-lead

In the many publications on ancient bronzes, sulphur has received little attention and usually is not analyzed for. It came as a surprise for us to find that ten of our twelve bronze objects contained significant amounts of sulphur. We therefore decided to expand our range of synthetic alloys to include several sulphur-containing series, of which we here report a few in order to demonstrate their mechanical and structural properties as a function of deformation and annealing.

The alloys A, B, C, and D were chosen to represent alloys which were typical of ancient compositions (table 1). They were melted under a cover of charcoal and cast in dry sand moulds in the shape of long bars, 50 × 5 × 1 cm, fig. 10. The cast alloys were allowed to cool to room temperature in the moulds.

The bars were cold-worked and annealed, and one

Table 1	Cu	Sn	S	Pb	Charge weight, kg	Temp. at pouring	Vol.% δ-phase as cast	Vol.% δ-phase annealed 120 min /700 °C
A	91.0	7.0	1.0	1.0	3.7	1300 °C	1	0
B	85.5	14.0	0.5	0	3.9	1200 °C	15	10
C	88.5	11.0	0.5	0	3.7	1160 °C	11	<0.5
D	92.5	7.0	0.5	0	3.6	1160 °C	1	0

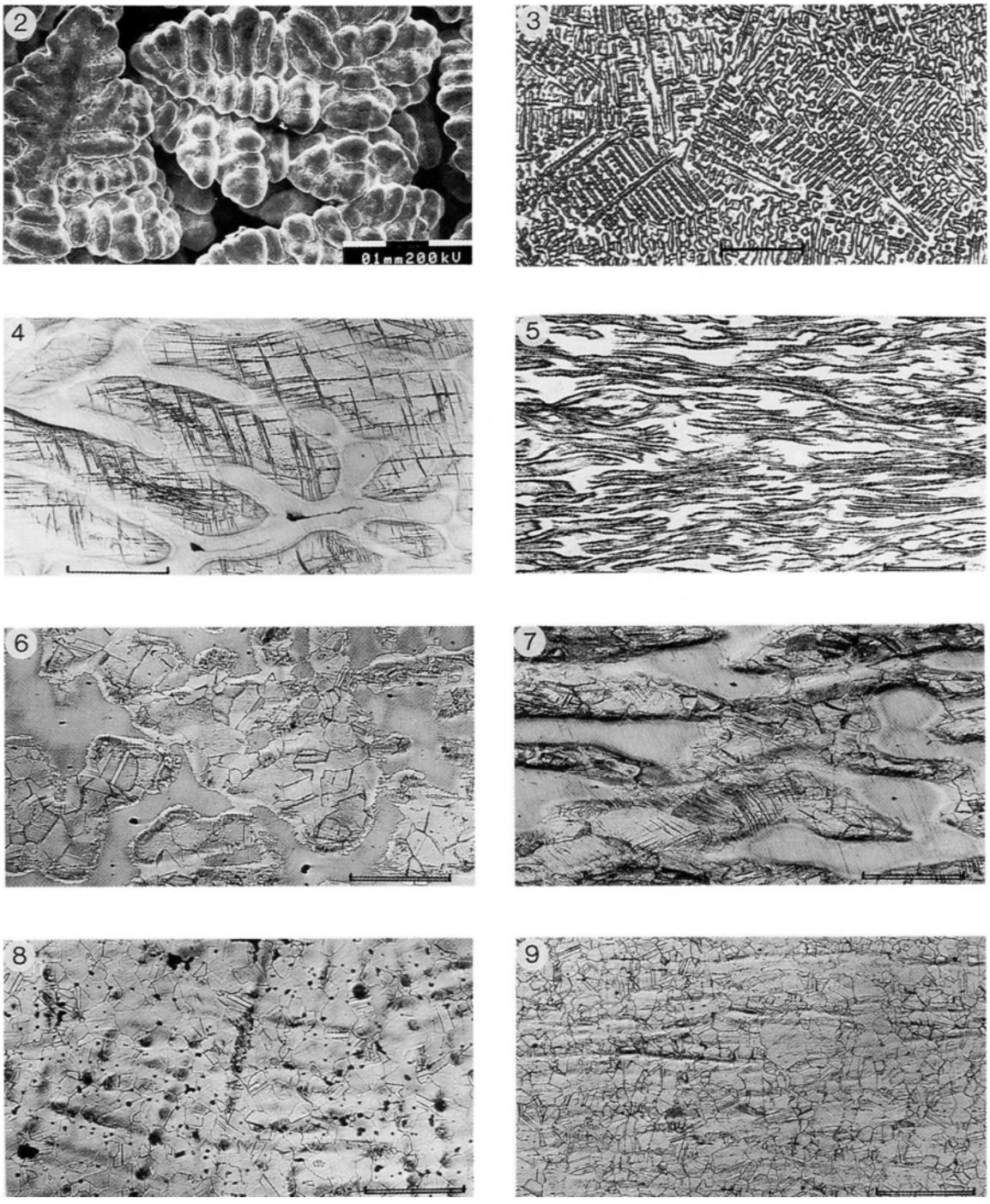

Figs. 2–9. The structure of a Cu-6Sn alloy in cast and worked conditions. Fig. 2. SEM picture of dendrites in the cast alloy. Scale bar 0.1 mm. Fig. 3. Polished and etched sections of a dendritic, cast structure. Scale bar 0.3 mm. Fig. 4. Cold-worked 44%: Slip lines in the segregated, cast structure. Scale bar 0.1 mm. Fig. 5. Cold-worked 81%: The cast structure has been severely deformed. Scale bar 0.3 mm. Fig. 6. Cold-worked 25% and recrystallized 50 min/550 °C. Scale bar 0.2 mm. Fig. 7. Cold-worked 63%, recrystallized 50 min/550 °C and again cold-worked 70%. Scale bar 0.1 mm. Fig. 8. Homogenized 120 min/620 °C, cold-worked 21%, and recrystallized 50 min/550 °C. Scale bar 0.2 mm. Fig. 9. Homogenized 120 min/620 °C, cold-worked 88%, and recrystallized 50 min/550 °C. Scale bar 0.2 mm.

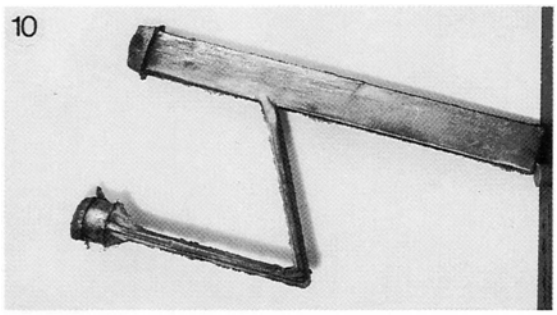

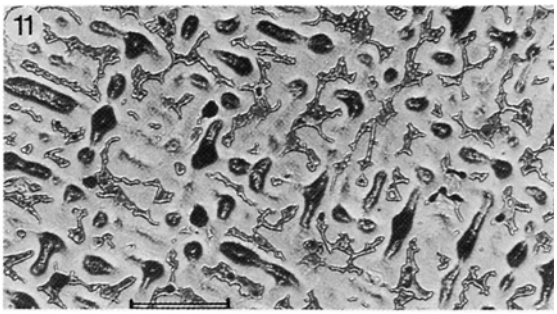

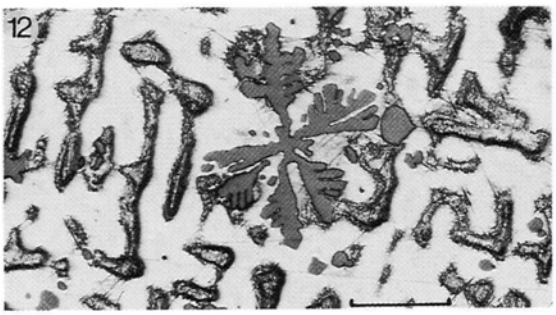

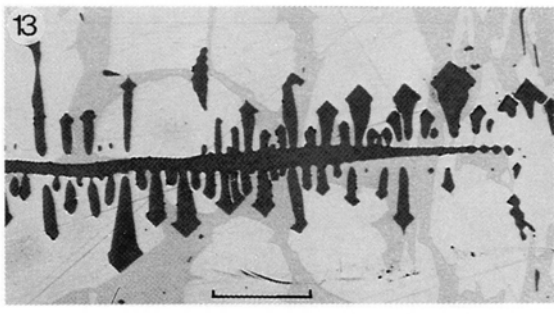

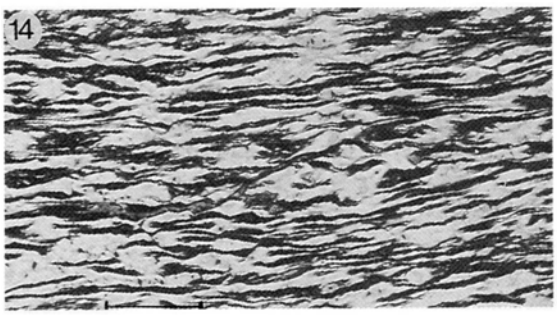

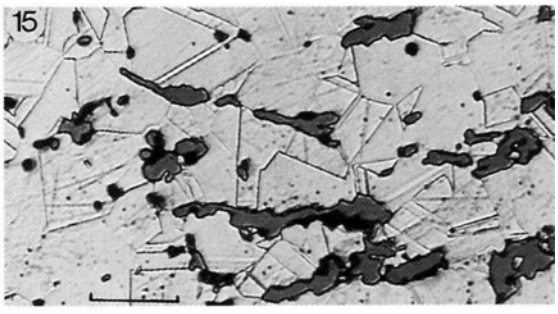

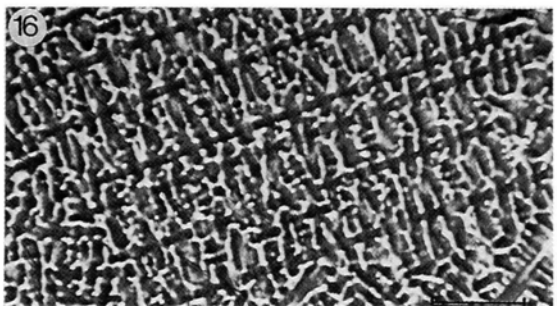

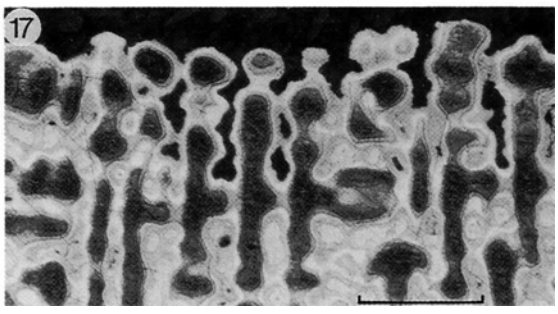

Figs 10–17. Fig. 10. Experimental bronze sample, cast in a sand mould. The rectangular part is 50 cm long. Fig. 11. The segregated structure of a cast 14Sn-0.5S alloy (alloy B). Scale bar 0.3 mm. Fig. 12. Palmate Cu_2S-inclusions in a cast 10Sn-1S alloy. Scale bar 50 μm. Fig. 13. Faceted Cu_2S-inclusion in a cast 20Sn-1S alloy. Scale bar 50 μm. Fig. 14. Segregated 11Sn-0.5S alloy (alloy C), cold-worked 78%. Scale bar 0.3 mm. Fig. 15. Alloy A (7Sn-1S-1Pb) cold-worked 35%, then recrystallized 120 min/700 °C. Elongated sulphides, black lead globules, and recrystallized α-grains. Scale bar 0.2 mm. Fig. 16. Cu-1As alloy, as cast. Regular, segregated (=cored) dendrites. Scale bar 0.3 mm. Fig. 17. Cu-8Sn-1As alloy, as cast. Cored dendrites at the surface give the alloy a whiteblue luster. Scale bar 0.1 mm.

alloy was hot-forged. Typical structures are shown in figs. 11–15.

In fig. 18 are presented some of the results in terms of Vickers hardness at a load of 5 kg. The top curve gives the maximum hardness obtained on alloy D. The δ-rich alloy B could only be cold-worked to a reduction of 48% before it suffered cracking.

Comparing alloy A and D, which have the same tin content of 7%, it was evident that the sulphur and lead rich alloy A was less ductile than D. However, it was quite surprising to find that both copper sulphide-rich alloys could be substantially cold-worked without breaking. The copper sulphide is clearly sufficiently ductile to follow the deformation of the metal phases. In the cast alloys the sulphides are homogeneously distributed as palmate, sub-angular particles, fig. 12, but during cold-work they attain elongated shapes and become arranged along parallel lines. This is particularly easily seen when the alloys are reheated to recrystallization after cold-work, fig. 15.

Comparing alloys B, C, and D, which only differ in tin

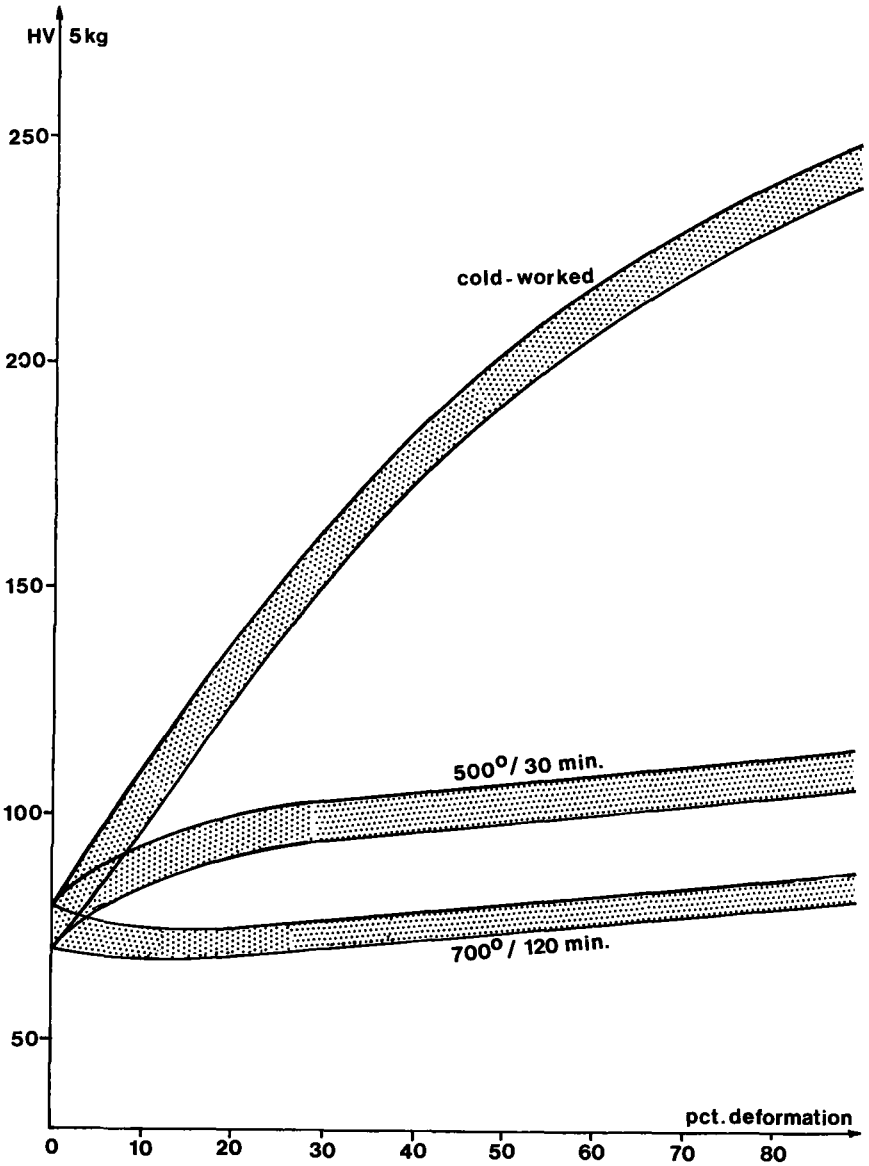

Fig. 18. Vickers hardness (5 kg) of a Cu-7Sn-0.5S alloy (alloy D). Cold-worked as shown, then recrystallized 30 min. at 500 °C. After thorough annealing for 2 hours at 700 °C, the hardness reaches its lowest level, the fully annealed state.

content, and thus in amount of δ-phase, it was observed that all can be cold-worked to hardnesses in the range 200–250 Vickers. This hardness range (and strength range) is the same as that found in low-carbon steels that have been worked or annealed, but not quenched in water. The properties of bronzes are, in general, not inferior to those of low-carbon steel. However, one weakness of the bronze alloys is their inherent porosity which stems from the shrinkage upon solidification. A bronze object hot- or cold-worked to final shape would be much superior to the equivalent cast object, because the subsequent reduction by working closes the numerous shrinkage cavities. Ancient iron and steel, on the other hand, has no shrinkage porosities, because the material was never melted but was produced by the direct process. Instead slag stringers occur, stretched in the forging direction and incurring fiber texture, which means that most iron objects have widely different mechanical properties in the longitudinal and transverse direction.

On annealing, i.e. reheating well above the recrystallization temperature of 300–400 °C for minutes or hours, the bronzes recover their basal hardness and strength, the material recrystallizes, and any heterogeneity resulting from casting is eliminated. Since this is a diffusional process, the final result depends very much upon the actual temperature and time applied. It will be noted that the hardness after annealing is almost independent of the foregoing cold-work, fig. 18. However the grain size of the recrystallized alloys decreases significantly, typically diminishing from about 200 μm to about 20 μm.

The lowest hardness of any bronze alloy is obtained by the following sequence: Casting, homogenization anneal, cold-work to a reduction by 10–20 %, followed by a thorough recrystallization anneal at about 700 °C for a few hours.

Copper-arsenic and copper-arsenic-tin

There are rather few data available on the properties of copper-arsenic alloys (Hanson & Marryat 1927; Maréchal 1958; Böhne 1965; McKerrell & Tylecote 1972; La Niece & Carradice 1989). Here we can present data referring to the synthetic alloys prepared during this project. The series covered the range 0–8 wt.% As, and other series within the ternary Cu-As-Sn system. The alloys were examined as cast and as homogenized, and in hot-forged, cold-worked and recrystallized conditions. Selected results are presented in figs. 16, 17, 19, 20.

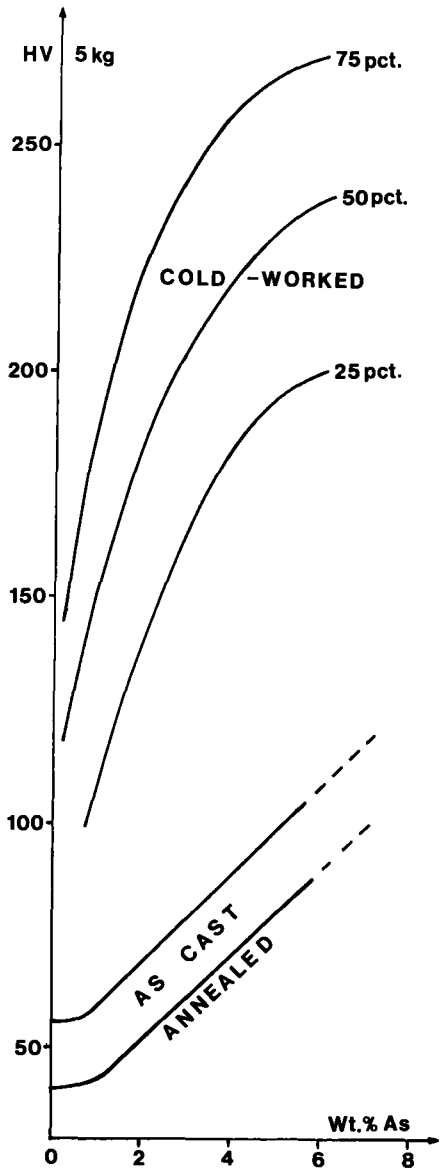

Fig. 19. Vickers hardness (5 kg) of Cu-As alloys. Below, the band for cast or annealed objects, compare Fig. 1. Above, the increasing hardness of cold-worked alloys. Arsenic is, on a weight percent basis, a far better hardening agent than tin.

Our results confirm the general opinion that copper is significantly strengthened by the addition of arsenic. The hardness of the annealed 4 wt.% As alloy is 70 ± 5 HV, while the annealed 4 wt.% Sn alloy is only 55 ± 5 HV. Evidently on a weight-percentage basis arsenic is a significantly better element than tin for hardening.

The difference becomes more pronounced when the alloys are cold-worked, compare the upper curves of figs.

19–20 with fig. 1. A Cu-2 wt.% As alloy is rather easily worked to a hardness of 225 HV (75% deformation), while a Cu-2 wt.% Sn alloy, even with the greatest deformation possible, will not increase above 190 HV. In order to confer a Cu-Sn alloy a hardness of 225 HV by 75% deformation, it is necessary to increase the tin content to 7 wt.%.

On annealing or recrystallizing, the hardnesses of Cu-As alloys fall back to the lower band, fig. 19. Prolonged maintenance of increased temperatures results in soft alloys close to the lower limit of the band, compare also fig. 18.

In one of our experimental series on the ternary Cu-As-Sn system, arsenic and tin were added in equal amounts, in consequence of which the abscissa in fig. 20 gives the sum of As + Sn as a wt.%. Thus, at 4 we have an alloy with 2 wt.% As and 2 wt.% Sn, and its hardness cold-worked to 50% is 200, while its hardness as fully recrystallized and/or annealed has decreased to 70.

It is evident that cold-work has most effect on the Cu-As alloys, somewhat less effect on the ternary Cu-As-Sn alloys, and least effect on the Cu-Sn alloys.

As more and more tin and arsenic are added to the alloys, new phases develop, such as $Cu_{31}Sn_8$ and Cu_3As. No ternary compounds exist, however, according to the equilibrium diagram by Maes & Strycker (1966). The new phases stiffen the alloys, which become harder and less ductile and thus difficult to shape by cold-working. Alloys with more than 4% of both Sn and As are rarely observed, and these "rich" alloys have not been further examined here.

The colour of arsenical bronzes changes to bluish-white by the time 2–4% As is added. Inverse segregation on casting is not uncommon, and the arsenic-rich dendrites at the surface convey a bluish-white lustre to the object, fig. 17.

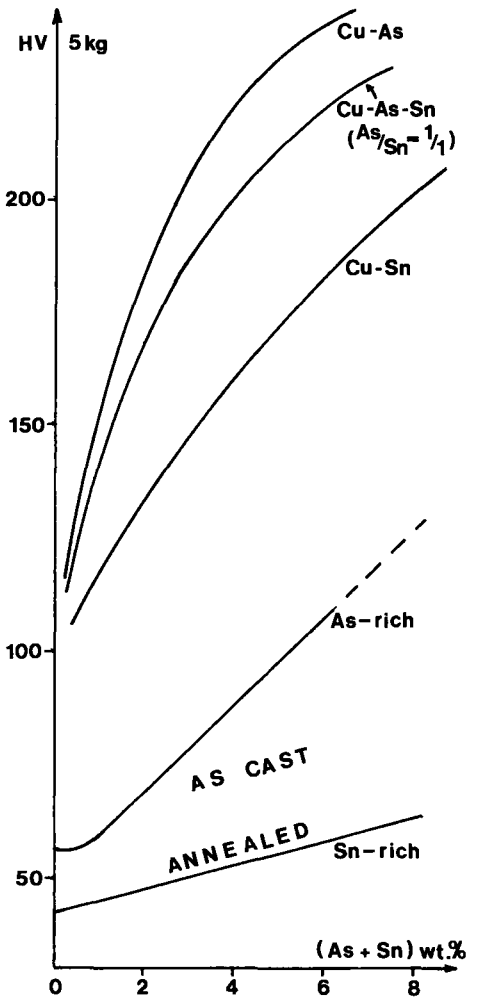

Fig. 20. Vickers hardness (5 kg) of Cu-Sn, Cu-As, and Cu-As-Sn alloys, annealed, and cold-worked 50% (the upper curves). Only one curve is shown for ternary Cu-As-Sn alloys, namely for those having the ratio 1:1 (weight) of arsenic and tin, and having been cold-worked 50%.

Complex alloys

Some of the ancient bronze objects are rather simple binary alloys, such as Cu-As and Cu-Sn, and the hardness diagrams presented here may then be used directly to estimate the degree of cold-work which has been applied to the cutting-edge of a knife or an axe. However, most bronzes are ternary or more complex alloys, and then the hardness diagrams may only serve as a guide. Usually the addition of extra alloying elements will increase the hardness, but there are no simple laws for prediction of the final hardness and strength. For example, while the annealed 7% Sn bronze has a hardness of 60, and the annealed 3% Sb bronze has a hardness of 60, the ternary annealed alloy 7% Sn – 3% Sb has a hardness of 95. Another example is that while the annealed 10% Sn bronze has a hardness of 70, and the annealed 2% As bronze has a hardness of 50, the annealed ternary 10% Sn – 2% As has a hardness of 90.

However the curves have turned out to be quite useful as a guideline for the minimum hardness in the annealed state and the maximum hardness in the cold-worked state, also for complex bronze alloys.

THE ARTIFACTS

Ten axes and two lurs were examined. The axes had previously been analyzed by Junghans et al. (1968) and we give the serial number in their table. None of them had been examined metallurgically before. The objects are grouped in their expected order of archaeological age as estimated by D. Liversage (pers. comm.).

Two wedge-shaped samples were removed from each axe, one taken from the cutting-edge (A) and one taken from the side going as far in as the middle (B). Analytical work showed that the two places had the same chemical composition within the experimental error. However, as will be shown, their metallography and strength were usually quite different due to different working.

Generally, all etching was performed with standard copper-ammonium chloride solutions, although in some instances supplementary information was acquired by applying alcoholic ferric chloride.

No. 1. B 2926. Tongue-shaped axe; Kirke Skensved Sogn; Tune Herred; Copenhagen Amt. Probably 4th millennium B.C. Weight: 135 g. Figs. 21–24. Table 2.

The tongue-shaped object measures 100 × (25–35) × 8 mm, where the first figure in the parenthesis is the width at the neck and the second the width at the cutting-edge. The last figure is the maximum thickness. At section B one side is slightly convex, but rather smooth, the opposite is flat, but has a wrinkled and warty surface. We propose that the object was cast horizontally in an open mould, and that the slightly convex part was the underside. A linear, 24 mm long raised excrescence on this side apparently is the impression of a defect, a crack, in the mould, fig. 21 (Aner & Kersten 1973, No. 520).

Corrosion is slight, only thin 10–30 μm copper oxides of olive-brownish to black colors are present.

Analytically, the tongue-shaped axe is a copper-arsenic alloy. The spectrographic and the EDAX-analyses agree well. The composition falls in the Bygmet-group, proposed by Liversage & Liversage (1989):

Sn 0 or trace
As 0.1–2 %
Sb ≤ 0.15%
Ag ≤ 0.05%
Ni ≤ 0.04%
Pb, Bi and Co not defined.

The polished sections show a red alloy with a number of fine, complex inclusions, 2–10 μm across. They consist, as in axe No. 2, of subangular copper oxides, Cu_2O, enveloped by lead- and copper-lead arsenates. Antimony and sulphur are not present. The inclusions date back from the smelting operations. In the cutting-edge they have acquired an elongate shape, suggesting some slight working, fig. 24. Junghans et al.'s spectral analysis was sensitive enough to reveal the bulk presence of 0.07 wt.% lead. Our energy dispersive method is not sensitive enough to catch the bulk value, but has, on the other hand, pinpointed the location of the lead to the slag minerals.

The etched sections show significant coring, overlapped by recrystallized, equiaxed α-grains with twins. The cutting-edge, A, displays a maximum hardness of 97, falling to 76 further inwards, with recrystallized grains 30–60 μm in diameter. The interior (B) displays hardnesses of 66–76, reflecting the segregated structure, and has recrystallized grains 100–200 μm in diameter, fig. 23.

This axe is only very slightly worked. The microporosities remain, except in the edge which also is the hardest part. Annealing was not very thorough, since the coring was not eliminated, and the hardness remained on a comparatively high level of 66–97. This level is, in fact, very high for a Cu-1% As alloy in which only very minor traces of cold-work can be detected in the microscope. It may be speculated that some kind of age-hardening has occurred, but it will require a detailed electron-microscopic study for this problem to be solved. Concluding, it appears that B 2926 was produced from a sulphide-free, lead-arsenic-enriched gossan-type ore, which yielded

Table 2

	Sn	S	Fe	Ni	Zn	As	Ag	Sb	Pb	Cu	Vol.% Sulph.	Vol.% Lead
J.1968; no. 8163	0	–	0	<0.01	0	1.05	<0.01	0	0.07	–	–	–
This work	<0.1	<0.1	<0.05	<0.05	<0.05	1.4	<0.1	<0.1	<0.1	(98.4)	0	0

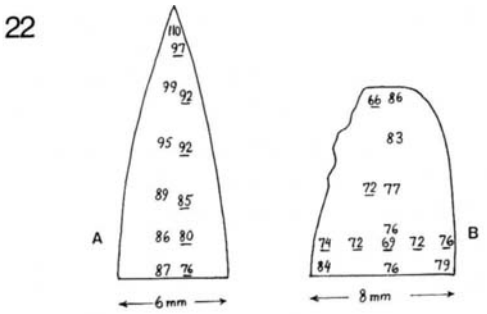

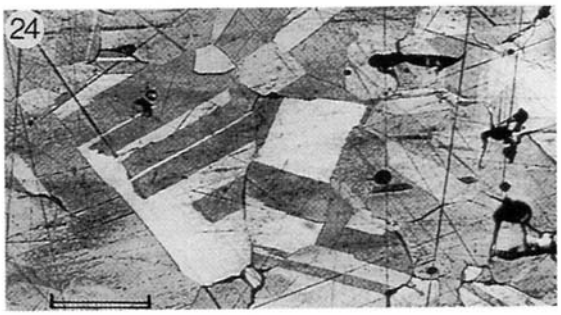

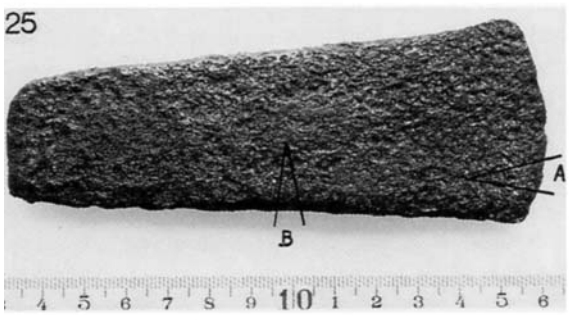

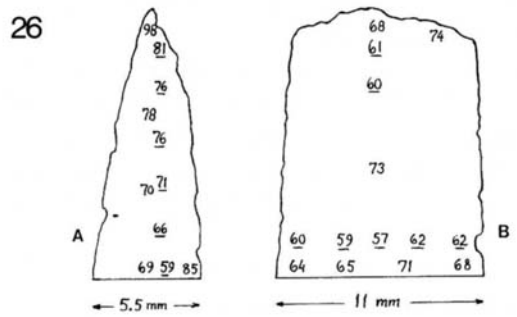

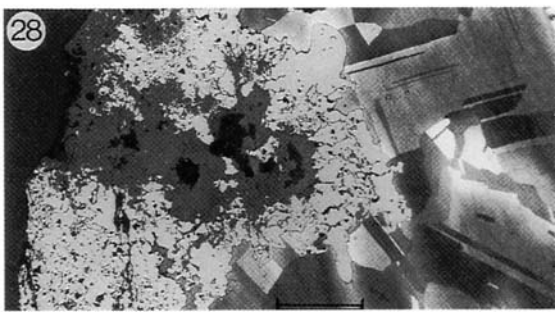

Figs. 21–28. Fig. 21. *No. 1. B 2926*. Tongue-shaped axe, 135 g. At D, a small ridge, suggesting a defect in the mould. Fig. 22. The Vickers hardness (5 kg) underlined, and the Microvickers hardness (100 g), sections A and B. Fig. 23. Slightly worked and recrystallized structure at B. Scale bar 0.3 mm. Fig. 24. Recrystallized and twinned grains at A. Elongated copper oxides with some lead-arsenates. Scale bar 20 µm. Fig. 25. *No. 2. B 5556*. Thin-butted flat axe. 311 g. Fig. 26. Vickers (5 kg) and Microvickers (100 g) of sections of A and B. Fig 27. Parallel ghost-lines on section A, suggesting forging. Scale bar 0.2 mm. Fig. 28. Two different corrosion products on the recrystallized Cu-As alloy: Red Cu_2O (light grey), with a pocket of arsenic-enriched green carbonate (dark grey). Scale bar 0.1 mm.

metal of Bygmet-composition. The object was cast and never remelted, since repeated melting (under oxidizing conditions) would have removed all the complex arsenates as scum.

Considering the unsymmetrical shape, the raw finish and the very limited work applied to the object, it may be suggested that B 2926 was traded from Central Europe as a semi-manufacture suited for remelting and the production of other objects.

No. 2. B 5556. Thin-butted flat axe. Denmark. Unknown locality. Probably 4th millennium B.C. Weight: 311 g. Figs. 25–28. Table 3.

The axe measures 130 × (28–48) × 12 mm. The two "flat" sides are symmetrical and slightly convex. Corrosion is rather heavy, the surface being irregularly coated by an inner red Cu_2O-layer and an outer green patina, each about 50 µm thick. There are numerous corrosion pits, generally 1 mm across, but locally up to 3 mm in diameter. Comparison of the two corrosion products reveals that arsenic is enriched in the green patina, but absent in the red copper oxide, fig. 28.

Analytically, the flat axe is a copper-arsenic alloy. The spectrographic and EDAX-analysis agree well. The composition falls within the range defined by Liversage & Liversage (1989) as Bygmet alloy, a composition which is typical for a significant number of flat axes found in Denmark.

The polished sections show a red alloy with a number of fine inclusions, 5–15 µm across. They are complex, consisting of two different phases in varying proportions. The central, angular part is blue, but red under crossed polars; it consists of Cu_2O. The exterior envelope is blackish grey, and has internal reflections under crossed polars. Energy dispersive point analysis shows that these envelopes consist of lead arsenate, lead-copper arsenate, and lead antimonate. The inclusions are not caused by corrosion but date back to the smelting operations. No sulphides are present.

None of the bulk analyses revealed any lead or antimony. These two metals can however be estimated by planimetry of the inclusions to sum up to less than 0.1 wt.% in the bulk.

Sample A from the cutting edge shows equiaxial α-grains with distinct twin structure and grain size of about 60 µm. Towards the interior the grain size increases to 100 µm. There is a system of parallel "ghost" lines on the etched section, fig. 27, that suggests previous heavy cold-work, followed by annealing. Correspondingly, the hardness decreases from 81 at the edge to 59 in the interior, where the reduction by hammering was quite insignificant.

Sample B represents cast and slightly worked, then annealed metal, with hardnesses of about 60. The segregation from casting is not entirely eliminated. The α-grains are equiaxed with twins and display grain sizes of 80–250 µm.

The observations indicate that the axe was cast vertically in a bivalve form. Any ribs or casting flashes at the joins of the two valves have been removed by hammering and possibly by grinding. While the subsequent working of the massive part was small and superficial, the cutting edge was reduced significantly, probably to a hardness above 100. The final annealing was stopped at hardness levels of about 80, well before the low equilibrium values of 40–45 were reached (fig. 19). Recrystallization occurred but sufficient hardness and strength remained in the axe. It is not clear whether some age-hardening has occurred.

Although the lead and antimony content is very low, it appears that the ores were derived from the oxidized arsenic-lead-antimony enriched gossan of some sulphidic ore crop. Since the slags are still present in the final axe, it appears that this particular metal was melted no more than once, and thus probably cast in its area of production in Central Europe. The origin of No. 2 would thus be very similar to that of the tongue-shaped object, No. 1.

Table 3

	Sn	S	Fe	Ni	Zn	As	Ag	Sb	Pb	Cu	Vol.% Sulph.	Vol.% Lead
J.1968; no. 8348	0	–	0	<0.01	0	0.33	tr.	0	0	–	–	–
This work	<0.1	<0.1	<0.1	<0.05	<0.05	0.47	<0.1	<0.1	<0.1	(99.3)	0	0

No. 3. B 1094. Low-flanged axe. Pederstrup, Ballerup Sogn, Smørum Herred, Copenhagen Amt. Early 2nd millennium B.C. Weight: 190 g. Figs. 29–32. Table 4.

The axe measures 110 × (22–50) × 8 mm and was probably cast edge down, in a bivalve mould. Superficial hammering has sharpened the edge, removed casting flashes and enlarged the flanges by plastic deformation. The flanges are now up to 12 mm wide. The cutting edge is oblique, suggesting that the axe at some time has been sharpened. In antiquity the axe was severely bent so that two deep cracks developed, 7 mm deep from one side, and 15 mm deep from the opposite side (Aner & Kersten 1973, 99). Corrosion penetrates the cracks and has raised a number of blisters on the otherwise flat surfaces.

Analytically the axe is a sulphide-containing copper-silver-arsenic-antimony alloy, which corresponds with the Ösenring compositions proposed by Liversage & Liversage 1989 (p. 64). It belongs to the half of the Danish finds of this composition having less than 1% tin.

Ösenring composition: As ≥ 0.4%
Sb ≥ 0.6%
Ni ≤ 0.2%
Sn ranges from 0 to 8%

The polished sections show a red to yellow alloy; evidently, even the small silver, arsenic, and antimony content is sufficient to turn the red copper to yellowish shades. For the first time we have an alloy with sulphides, about 0.4 vol.%, suggesting that the ores from which the Ösenring metal was produced was partly sulphidic, partly oxidic. The sulphides, Cu_2S, occur as minute (2–10 µm) blue blebs, distributed at random, deformed, however, by the cold-work applied to the cutting-edge and flanges.

The etched sections show a cast structure in which coring is not fully eliminated, fig. 31, and in which a number of 0.1–0.3 mm micropores occur. The bulk of the sample shows equiaxed, recrystallized grains, 100–300 µm across, with a few twins and a hardness of 55 ± 3, fig. 32. The flanges and the edge have been severely cold-worked, so that minute cracks have developed. The recrystallized grains are slightly elongated from some final cold-work, and the hardness ranges up to 90 in the very edge. The exterior 4 mm of the flanges have been affected by the hammering, judging from the combined hardnesses and appearance of the grains.

The axe has been cast as a flat object like No. 2, or with slight flanges. After casting, severe hammering, possibly both hot and cold, has raised the flanges, or at least the major part of them, and the edge has been sharpened. Under this action the material was exposed to the limits of its workability, as witnessed by the microcracks. After having been used, the axe suffered a violent bending which opened two large cracks, located almost at the transition from the exposed part of the axe to its mounting. It is difficult to explain these cracks, because the material is too strong and tough to break in this way under normal conditions, even given the number of large microporosities observed. The axe may indeed have been deposited after having been forcibly made useless.

No. 4. 11073. Low-flanged axe. Bygholm, Hatting Sogn, Hatting Herred, Vejle Amt. Early 2nd millennium B.C. Weight: 480 g. Figs. 33–36. Table 5.

The dimensions of the axe are 155 × (22–70) × 13 mm. It is rather rough and uneven and has the poorest finish of the twelve objects examined. In the cutting-edge is a deep incision, probably damage from heavy blows. The flanges have been somewhat shaped by hammering to maximum widths of 15–16 mm. Corrosion is uneven, generally composed of a thin, inner green patina (≈ 30 µm) and a thick, outer reddish oxide (0.2–0.6 mm). Local irregularities, especially near the butt, may result from poor casting technique.

Table 4

	Sn	S	Fe	Ni	Zn	As	Ag	Sb	Pb	Cu	Vol.% Sulph.	Vol.% Lead
J.1968; no. 8271	0.01	–	0	0.08	0	0.6	0.4	0.69	0	–	–	–
This work	<0.1	0.11	<0.05	0.08	<0.05	0.50	0.9	0.4	<0.1	(97.8)	0.4	0

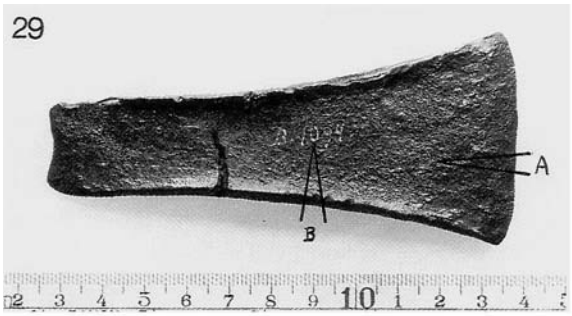

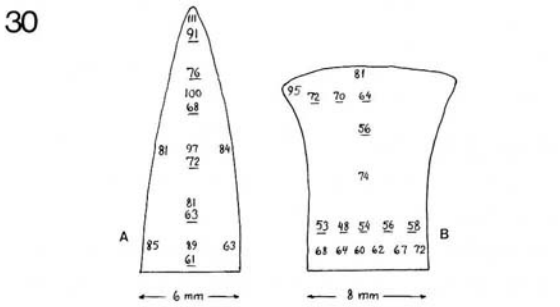

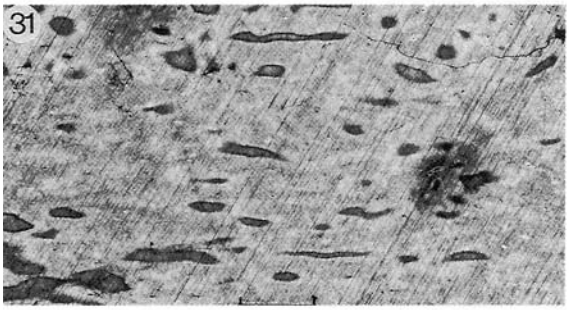

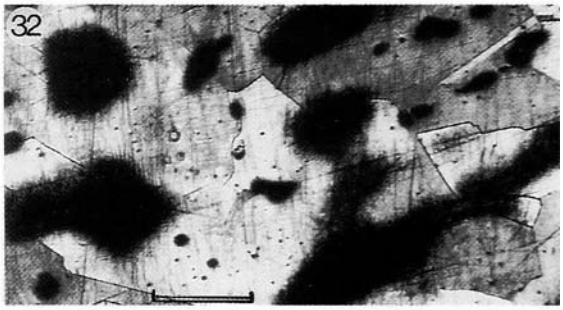

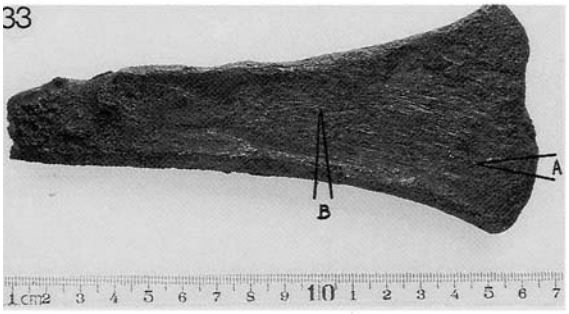

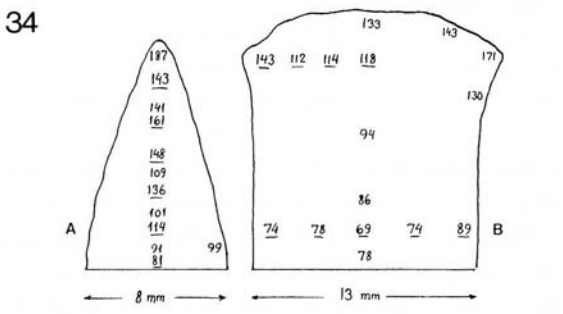

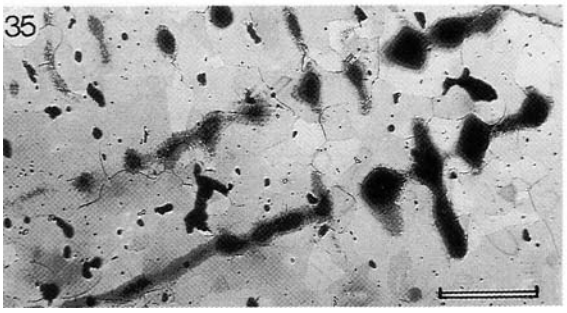

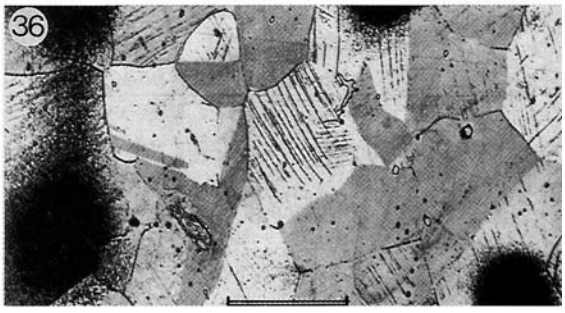

Figs. 29–36. Fig. 29. *No. 3. B 1094*. Low-flanged axe, 190 g. Fig 30. Vickers (5 kg) and Microvickers (100 g) hardness of sections A and B. Fig. 31. Segregated and worked structure at A with microcrack (above right). Scale bar 0.5 mm. Fig 32. Cored and recrystallized grains in the interior of B. Scale bar 0.1 mm. Fig. 33. *No. 4. 11073*. Low-flanged axe. 480 g. Fig. 34. Vickers (5 kg) and Microvickers (100 g) hardness of sections A and B. Fig 35. Cored and recrystallized grains in the interior of B. Scale bar 0.5 mm. Fig. 36. Recrystallized and cold-worked material in flanges of B. Scale bar 0.2 mm.

Table 5											Vol.%	
	Sn	S	Fe	Ni	Zn	As	Ag	Sb	Pb	Cu	Sulph.	Lead
J.1968; no. 8260	1.95	–	tr.	0.71	0	0.71	0.53	0.99	0	–	–	–
This work	2.1	0.15	<0.05	0.74	<0.05	0.36	0.74	0.82	<0.1	(95.0)	0.5	0

The axe represents the first tin bronze metal appearing in Denmark about 2000 B.C., in the late Neolithic. The alloy is sulphide-rich and rather complex. It belongs in the Singen group as defined by Liversage & Liversage (1989:59):

Singen metal: As ≥ 0.1%
Sb ≥ 0.5%
Ag ≥ 0.3%
Ni ≥ 0.4%

The tin content in objects of this group varies between 0.01 and 10%, but 78% of the examined samples had like the present object less than 2% Sn. (Liversage 1989: graph 9).

Polished sections are yellow with a reddish tint. There are numerous tiny, blue copper sulphide inclusions, about 0.5 vol.%. They are softly rounded or palmate-lobed, and in the worked cutting-edge they are plastically deformed and rotated into the directions of forging. They are generally 5–10 μm across, but reach sizes of 25 μm. There are only a few microporosities from the casting, and they are rather small, ≈ 25 μm across.

The etched sections display a coarse, cast structure in which coring has not been entirely eliminated, fig. 35. The dendrite arm spacing is about 250 μm, suggesting rather slow cooling. Also the coarse sulphides point in this direction. The comparatively slow cooling is due to the rather large mass of the axe. It now weighs 480 g, but may easily have weighed 50% more before gates and risers were trimmed away.

The bulk of the material consists of large, equiaxed grains, 100–300 μm across, with a hardness of 75 ± 6. The cutting-edge has been cold-worked to a distance of about 5 mm and now displays equiaxed grains, 30–100 μm across, with a maximum hardness of 161. The flanges have acquired their basic shape by casting, improved locally however by mild hammering. Here the grains are elongated and rich in slip-lines from cold work, showing a maximum hardness of 143, fig. 36.

The axe should be of about the same age as the previous axe, No. 3. It has been cast in almost its final shape and only limited working of the edge and the flanges has occurred. It is a tin alloy and has not been very thoroughly annealed after working, and therefore is significantly harder than No. 3.

Before deposition the blade was destroyed by a heavy blow. Perhaps we here have another example, like No. 3, of deliberate destruction ?

No. 5. 26073. Flanged axe. Vicinity of Silkeborg, Gjern Herred, Skanderborg Amt. About 1750–1500 B.C. Weight: 250 g. Figs. 37–40. Table 6.

The axe measures 159 × (21–58) × 9 mm. It is of elegant shape and well-preserved, with less than 20 μm thick copper oxides on the surface. The flanges have been worked after the casting so that they attain maximum widths of 13 mm. The cutting-edge has been worked on at least the exterior 11–12 mm, and the neck has been hammered over after removal of the casting gate. Minor bruises mar the cutting-edge.

Analytically, the axe is a sulphide-rich tin bronze of the Faardmet group (Liversage & Liversage 1989,67):

Faardmet As 0.25–1.8%
Sb 0.02–0.7%
Ag 0.01–0.16%
Ni 0.25–1.2%
4.3 < Sn < 13.3%

The axe belongs to the earliest part of the full Bronze Age in Denmark, and metallurgically represents the important change to full tin bronze alloys, whereby other elements decreased in importance. Unlike earlier, the tin is now systematically added. We agree with Liversage and Liversage (1989), who conclude from examination of the Danish artifacts with the Faardmet impurity pattern that "the consistency of the distribution suggests that the people who made the bronze knew exactly what tin content they wanted, even if they did not always hit it right". It is the general opinion that objects in this group are not

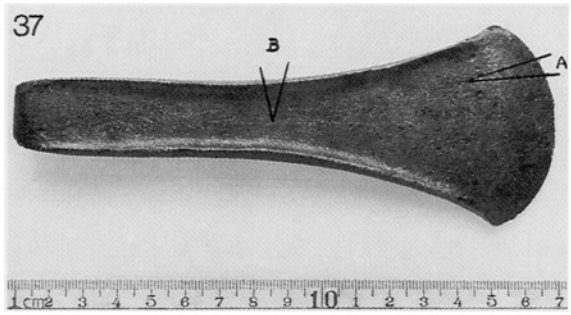

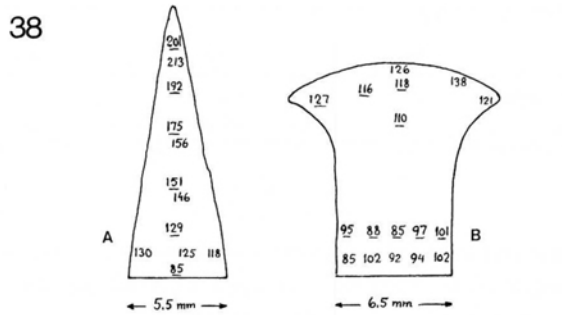

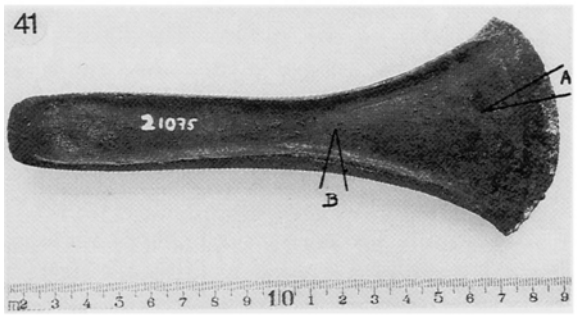

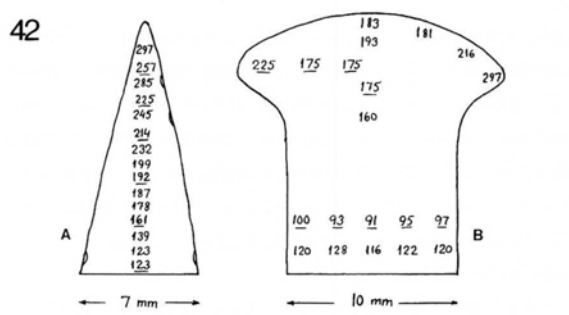

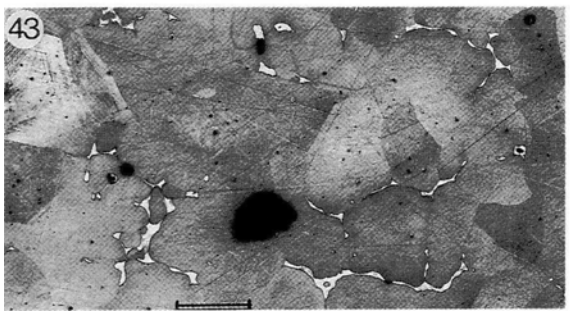

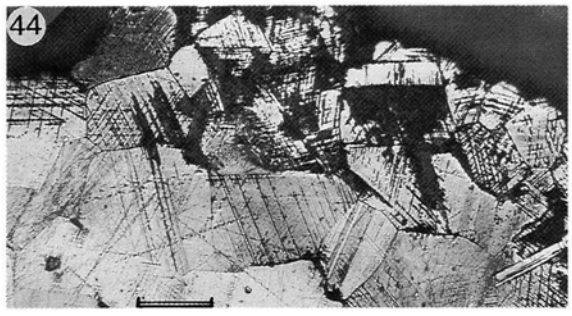

Figs. 37–44. Fig 37. *No. 5. 26073*. Flanged axe of elegant shape, 250 g. Fig. 38. Vickers (5 kg) and Microvickers (100 g) hardness of A and B. Fig. 39. Typical intercrystalline corrosion attack in medium-work-hardened tin bronze section B. Scale bar 0.1 mm. Fig. 40. Recrystallized and cold-worked grains with slip lines. Clusters of elongated sulphides. Scale bar 50 µm. Fig. 41. *No. 6. 21075*. Flanged axe, similar to No. 5, but larger. 354 g. Fig. 42. Vickers (5 kg) and Microvickers (100 g) hardness of A and B. Fig. 43. Interior of B, with significant remnants of δ-phase (white), probably stabilized by nickel. Scale bar 0.1 mm. Fig 44. Extremely cold-worked and hard edge, A, with slip line corrosion. Scale bar 0.1 mm.

Table 6											Vol.%	
	Sn	S	Fe	Ni	Zn	As	Ag	Sb	Pb	Cu	Sulph.	Lead
J.1968; no. 8434	6.4	–	tr.	0.3	0	1.1	0.08	0.22	tr.	–	–	–
This work	8.8	0.35	0.08	0.37	<0.05	>0.2	0.09	0.22	<0.1	(89.5)	1.6	0

imports, but were cast in Denmark (Brøndsted 1939, vol. 2, Vandkilde 1989).

The polished sections show a yellow alloy with numerous fine, blue inclusions, amounting to 1.6 vol.%. These were identified as the copper sulphide, Cu_2S, often with minor amounts of iron (0.5–0.8 wt.%). The sulphides are free of As, Sb, Sn, and Ni. They are typically 3–30 μm in size, and often form palmate and lobed figures. In the worked parts of the axe they have been plastically deformed and turned into parallel streaks. The massive part of the casting is rich in micropores. These have been closed by working both along the cutting-edge and to a depth of about 3 mm under the flanges.

The etched sections show that the original coring has been almost eliminated by annealing. In places a little δ-phase, 3–15 μm across, remains as rounded blebs. Evidently the original casting was quite rich in δ-phase, which gives support to the 8.8% value for tin. Repeated hammering and annealing have left the axe with a variety of structures. The cutting-edge itself displays fine, 15–30 μm, recrystallized grains, which are elongated and striated by cold-work to a hardness of 201. Inwards the recrystallized grains grow to 50–75 μm and the hardness drops to 85.

Also the flanges have been severely hammered and shaped. The parts near the surface display elongated sulphides and small, work-hardened, recrystallized grains and have a hardness up to 127. Below a depth of 3 mm, the porosities from casting reappear, the recrystallized grains are 30–75 μm across, and the hardness about 85.

The axe has been produced from sulphide-rich ores. The final melting probably took place under reducing conditions in a crucible covered by charcoal and the axe was cast edge down in a bivalve form. The axe is unusually rich in Cu_2S inclusions, which are sufficiently plastic to follow the displacement of the metallic matrix without breaking, during either hot or cold working. Repeated hammering and annealing have given the axe a cutting-edge with a maximum hardness of 200. 11 mm below the edge the hardness is that of the bulk material, 85. Similarly, the outer 3 mm of the flanges have been shaped by working after removal from the mould.

No. 6. 21075. Flanged axe. Kragebæk, Merløse Herred, Holbæk Amt. About 1750 B.C. or a little earlier. Weight: 354 g. (According to Aner & Kersten 1976, 109 Hørby Sogn, Tuse Herred). Figs. 41–44. Table 7.

The axe resembles the previous one, but it is heavier and larger, measuring 173 × (22–69) × 11 mm. The flanges have been worked and are up to 14–16 mm wide and somewhat unsymmetrical owing to differences in hot-working. The cutting edge is visibly sharpened on the last 12 mm by a combination of cold-working and grinding. The corrosion is not severe; however, locally pits 0.1–0.3 mm wide and deep, filled with green patina, are seen. The red copper oxide is almost absent. The slipbands from cold-working of the metal are still discernible as "fossil traces" in the green patina when examined in a polished section under the microscope.

Analytically, the axe is a sulphide-rich tin bronze belonging to the Singen group. Only silver is a little low. Except for the arsenic data, where we prefer the old determination, the analyses agree well.

The polished sections through the massive bulk show a yellow alloy with 0.1–0.3 mm wide micropores from casting. In the cutting-edge and flange parts all micropores have been closed by hammering. There are numerous sulphides, Cu_2S, but they are smaller than in No. 5 (2–20 μm) and fewer, adding up to about 0.6 vol.%. In the worked parts they have been rotated and become plastically elongated in the forging direction.

Etched sections display a cast structure in which coring has been almost eliminated by annealing. However, numerous δ-bodies appear everywhere, adding up to about 2 vol.%. In the interior which has only been little affected by the working, the recrystallized grains are equiaxial and 100–300 μm across, and the hardness is about 90, corresponding to an annealed tin-rich bronze (fig. 43). The cutting-edge and the flanges have been repeatedly worked and annealed. The last operation was a very heavy cold-working, leading to the extreme edge hardness of 257. The flanges have attained the somewhat lesser hardness of 225. The small recrystallized grains have here become flattened and display numerous slipbands, but no micro-

Table 7											Vol.%	
	Sn	S	Fe	Ni	Zn	As	Ag	Sb	Pb	Cu	Sulph.	Lead
J.1968; no. 8235	8	–	tr.	0.7	0	1.2	0.31	0.5	0	–	–	–
This work	8.8	0.15	<0.05	0.74	<0.05	>0.4	0.22	0.49	<0.1	(88.5)	0.6	0

cracks have opened. Grains near the surface are corroded along the slipbands in a very characteristic way, the blue grid consisting of copper oxides, Cu_2O, fig. 44.

A qualitative test was run with the SEM-EDAX equipment on the three different corrosion products which could be identified on the surface. The major one is a 50 μm thick, grey, outer crust, which is slightly rusty-red under crossed polars. It turned out to consist of major tin, iron and copper, and minor silicon, arsenic, and phosphorus. Oxygen, carbonate, and hydroxyl ions are no doubt present at a significant level.

The minor one, a discontinuous greenish layer, green under crossed polars, and up to 40 μm thick, contained major tin, copper, and silicon, and minor arsenic and chlorine. It appears to be a silicate, related to chrysokol.

Finally there occur 10–50 μm blebs of a whitish-grey oxide phase, disseminated through the grey and green phases. It is complex, displaying tin, copper, arsenic, silicon, iron, nickel, and chlorine. It may be unequilibrated gels, and is perhaps not a stoichiometric mineral.

Common to all corrosion products is the depletement of copper. While the weight ratio Cu:Sn is about 10 in the metallic matrix, it varies between 0.3 and 1.0 in the corrosion products. Evidently copper has been selectively leached and has disappeared into the adjacent soil. On the other hand, substantial amounts of iron, phosphorus, chlorine, and silicon have been introduced from the surroundings. All the corrosion products were sulphide-free.

The axe has been cast, edge down, and while the flanges may already have been moulded in the raw product, they have attained their final shape by hammering. Intensive hammering and annealing has certainly been necessary in shaping an alloy of this type. The final cold-work brought the edge to the maximum hardness for this alloy and the flanges to a somewhat lower hardness. The edge acquired its final faceting by grinding. The axe is a fine example of the skill of the early Bronze Age craftsman, being of a very elegant shape and simultaneously displaying superior technological properties.

No. 7. B 4077. Low-flanged axe. Moskjær, Virring Sogn, Sønderhald Herred, Randers Amt. About 1750–1500 B.C. Weight: 132 g. Figs. 45–50. Table 8.

The axe measures 110 × (18–46) × 10 mm, with up to 12 mm wide flanges. While the shape is quite common for flanged axes of the early Bronze Age, the corrosion is unusual. The heavy layer consists of an inner, 1 mm thick, black layer and an outer, up to 2 mm thick, blistery, black layer. The border between the two layers is smooth, fig. 46.

The following information can be extracted from the data of acquisition: "The axe was discovered by Knud Petersen, Moskjær, in 1888. It was found together with two flint sickles and some other flint material. The depth was 6 feet, and there were thick layers of peat underneath. About 100 feet distant the turf terminated against a sloping field under culture". Although not stated directly it must be concluded that the axe was found during turf-cutting and that the overlying soil also was of a peaty nature.

The axe has the most tin of those we have examined. The impurities of arsenic, silver, antimony, and nickel place it in the Faardmet group of the early Bronze Age. It is rich in copper sulphide, ≈ 2 vol.%, and also is the first to contain appreciable quantities of lead.

Polished sections show a yellow alloy with very many and distinct pin holes 0.1–0.3 mm across, resulting from solidification shrinkage. The holes have been closed by forging on the cutting-edge and under the flanges to a depth of 3 mm. The sulphides are 3–10 μm across and consist of Cu_2S. They are rotated and significantly deformed in the forged areas. The δ-phase occupies about 2 vol.%. Lead appears as fluffy, dark blebs, usually 1–5 μm across, which are associated with the copper sulphide or included as discrete blebs in the δ-phase.

Etched sections through the bulk show that coring is well preserved. This part is apparently not recrystallized, but only somewhat homogenized, because deformation

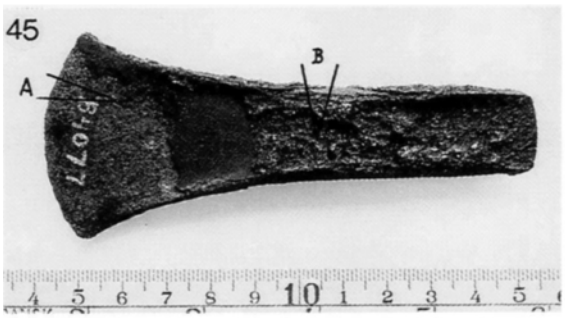

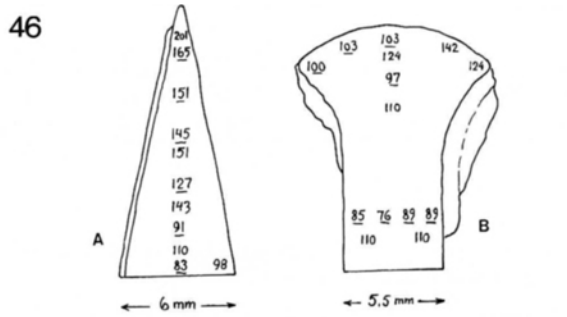

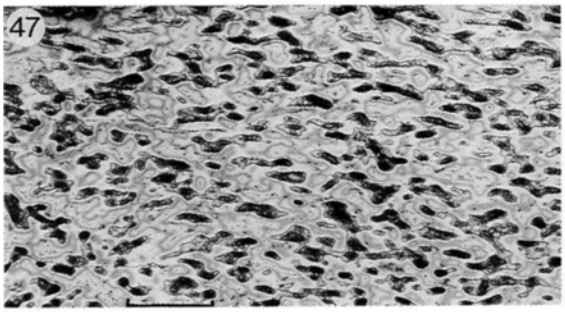

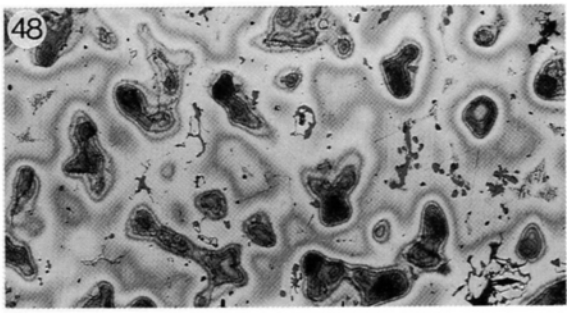

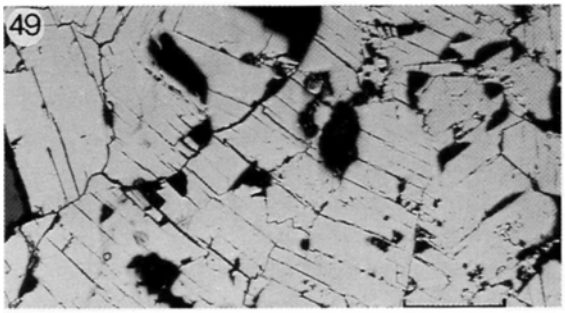

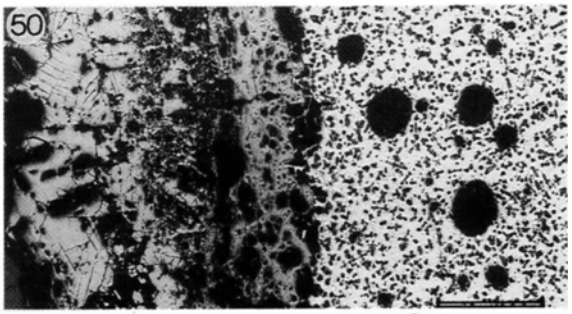

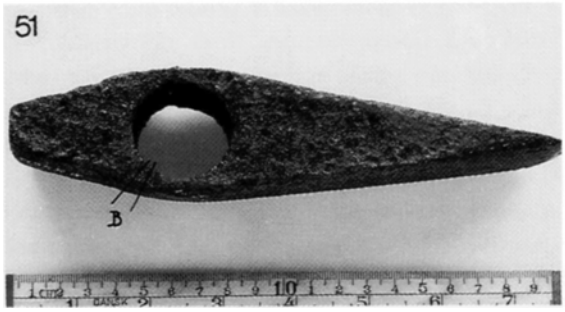

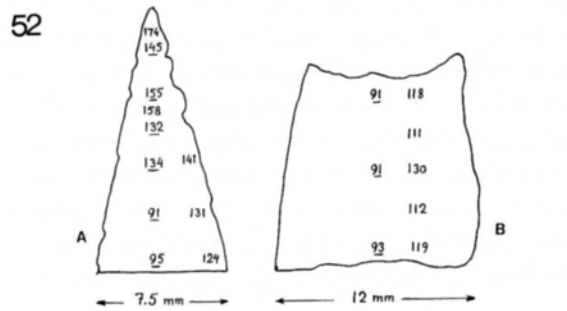

Figs. 45–52. Fig. 45. *No. 7. B 4077.* Low-flanged axe with thick layers of sulphides due to corrosion, 132 g. Fig. 46. Vickers (5 kg) and Microvickers (100 g) hardness of A and B. Fig. 47. Well-preserved coring, but somewhat deformed near the surface by working. Scale bar 0.3 mm. Fig. 48. The δ-phase and the sulphides are concentrated in the areas that solidified last. Interior of B. Scale bar 0.1 mm. Fig. 49. The exterior corrosion layer consists of Cu_2S with impurities of arsenic. Scale bar 0.2 mm. Fig. 50. A: Cu_2S corrosion layer. B: Complex corrosion layer. C: Dendritic bulk with major voids from the original casting process. Scale bar 1 mm. Fig. 51. *No. 8. B 5564.* Shaft-hole axe. 1470 g. Fig 52. Vickers (5 kg) and Microvickers (100 g) hardness of A and B.

Table 8	Sn	S	Fe	Ni	Zn	As	Ag	Sb	Pb	Cu	Vol.% Sulph.	Vol.% Lead
J.1968; no. 8191	10	–	tr.	0.32	0	1.15	0.05	0.17	0.68	–	–	–
This work	9.4	0.4	<0.05	0.37	<0.05	>0.4	<0.1	0.18	0.9	(88)	2.0	0.8

has been very minor, fig. 48. The hardness is correspondingly low and irregular, 84 ± 5.

The edge is worked to a distance of at least 20 mm. The recrystallized grains become finer and finer (10–20 μm across) the closer we come to the edge itself, where the maximum hardness is 165. Also the flanges are deformed, showing grains of about 50 μm and a maximum hardness of 103.

The exterior corrosion layer was probed by the EDAX-instrument and shown to be homogeneous copper sulphide, Cu_2S, with an impurity level below our detection limits except for 1–2 % As. The layer is well-developed, polycrystalline and anisotropic with a grain size of 0.2–0.5 mm and with distinct parting along crystallographic planes, fig. 49. It appears to be the low-temperature orthorhombic copper sulphide, Cu_2S, which is distinct from the high-temperature cubic digenite, Cu_9S_5 , which is so common in the matrix of most ancient copper objects and is derived from the smelting process.

The inner corrosion layer is a heterogeneous, porous material with major amounts of copper, tin, and sulphur, and minor amounts of arsenic, fig. 50. In this layer distinct δ-blebs, as yet undissolved, may be seen. The two corrosion products are different from those discussed on axe No. 6.

Summing up we meet here an axe which is not thoroughly mechanically worked and recrystallized. Only the cutting-edge and the flanges have been worked, as testified by oriented sulphides, closed micropores and fine recrystallization. The 9–10 % tin alloy has in itself sufficient strength and hardness and is also much less ductile than arsenic- and low-tin-copper alloys. The craftsman may have acquiesced with some local overworking and otherwise been satisfied with the properties as cast.

The axe was deposited in a lake or a peat bog and must have experienced about 3500 years under anaerobic conditions. Instead of the usual oxides, hydroxides, and carbonates, we here find an exterior solid Cu_2S layer and an interior complex Cu-Sn-As-sulphide.

No. 8. B 5564. Shaft-hole axe. Kragenæs, Birket Sogn, Lollands Herred, Maribo Amt. About 1750–1500 B.C. Weight: 1470 g. Figs. 51–62. Table 9.

This is the only shaft-hole axe in our selection. It is big, but rather primitive and without decoration. It measures 185 × (51–55) × 38 mm and has a slightly elliptical hole measuring about 33 × 30 mm, fig. 51. When viewed edge-on the axe appears rhomboidal (instead of rectangular) in cross section, and also the shaft-hole is imprecise. While one side is pretty flat, the opposite is rough and undulating (Aner & Kersten 1977,76). There are no indications of hammering.

Analytically the axe is a full tin bronze with significant contents of As, Sb, Ag, and Ni, placing it in the Faardmet group (Liversage & Liversage 1989,67). It is further important to note the content of sulphur, present as copper sulphides, and of iron and lead.

Polished sections show a yellow alloy with many pinholes and microporosities from the casting. They are 0.05–0.2 mm across and interdendritic with concave outlines, fig. 54. Neither under the flange nor along the edge have they been closed by working. The sulphides are rather large, up to 30 μm across, and of the usual rounded, lobate-palmate forms. The microprobe shows that they are Cu_2S, sometimes with significant amounts of iron in solid solution, typically 0.3–0.5 wt.%.

Table 9	Sn	S	Fe	Ni	Zn	As	Ag	Sb	Pb	Cu	Vol.% Sulph.	Vol.% Lead
J.1968; no. 8378	7.6	–	tr.	0.35	0	1	0.06	0.29	1.15	–	–	–
This work	8.4	0.23	0.12	0.46	<0.05	>0.4	0.16	0.28	1.2	(88.2)	1.0	1.0

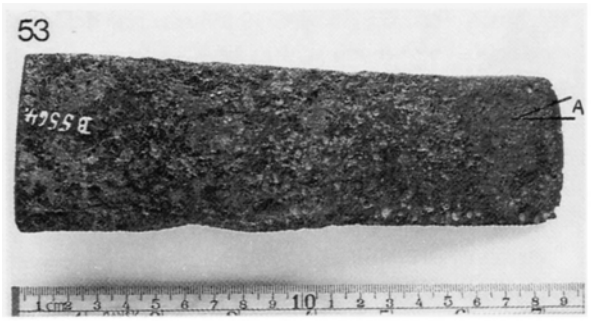

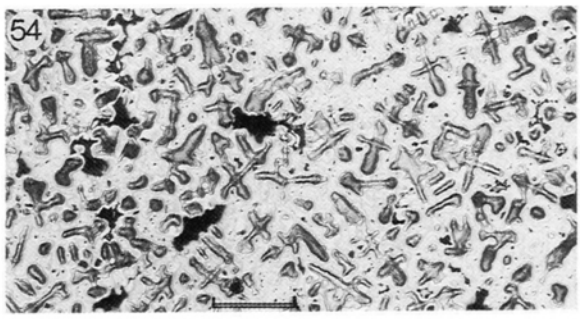

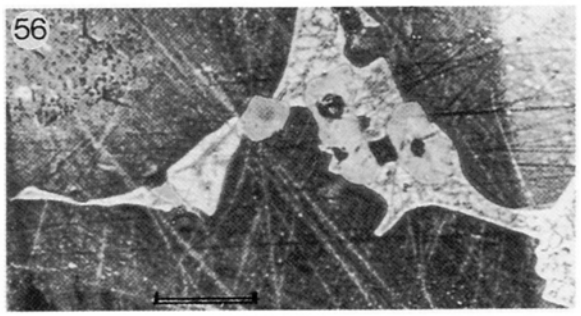

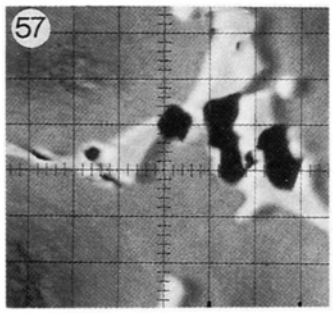

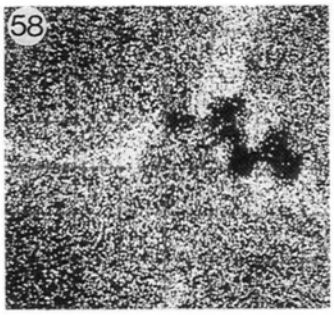

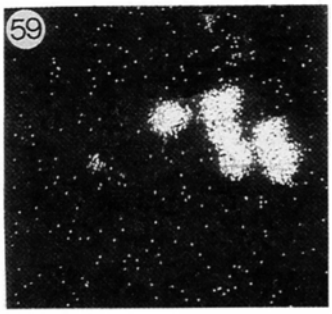

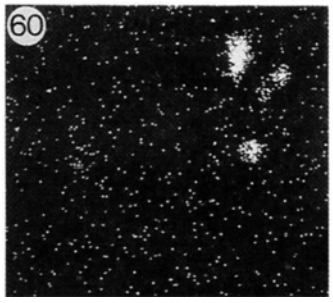

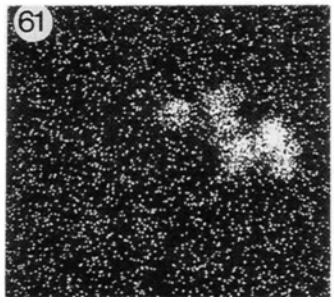

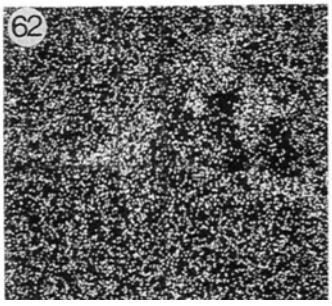

Figs. 53–62. Fig. 53. *No. 8. B 5564*. Shaft-hole axe, from the side. Fig. 54. Segregated, unequilibrated structure with short dendrites and interdendritic microporosities. Scale bar 0.3 mm. Fig. 55. Recrystallized α-phase and interdendritic δ-phase (white). Scale bar 0.2 mm. Fig. 56–62. Microprobe examination. Scale bar 20 μm. Fig. 56. δ-phase with inclusions. Fig 57. Back-scattered-electron (BSE) picture, showing the area under investigation. Fig. 58. Sn L_α radiation: Tin is concentrated in the δ-phase. Fig. 59. S K_α radiation: Sulphur is entirely located in the sulphides. Fig. 60. Pb L_α radiation: Small lead globules are associated with sulphides and δ-phase. Fig. 61. Fe K_α radiation: Iron is concentrated in the sulphide. Fig. 62. Ni K_α radiation: Nickel is concentrated in the δ-phase.

Etched sections display coring, showing a cast and unequilibrated structure. The δ-phase, the sulphides and the microporosities form interlacing networks which have not been modified by working, fig. 55. There is little recrystallization, but mainly the typical segregational structures, grading through various yellowish, brownish, and red colours. The lead occurs as discrete, fluffy blebs, 3–10 μm across and usually associated with the last melt to solidify, i.e. the present δ-phase and sulphides, fig. 60. The nickel is partitioned between the δ- and the α-phase, the ratio of nickel in the two phases being 3–4, fig 62. The hardness is 93 ± 5, somewhat irregular due to the coring. In general the etched sections appear "dirty", being rich in black filaments, that may derive from an improper casting process.

Only in the exterior 1 or 2 mm of the cutting edge can a little coldworking be identified. The material has recrystallized to 20–60 μm twinned grains, but the δ-phase and the sulphides are largely unaffected. The hardness increases to a maximum of about 150 at the very edge.

The patina is of a dark chocolate colour with green nuances. There are numerous corrosion pits, 1–5 mm across. In the complex, botryoidal corrosion crust, there are undissolved δ-phase and locally small blebs of copper, 2 μm or 25 × 2 μm, evidently re-cemented copper from seasonal variations in the corrosion process, the so-called destannification.

The axe with its oblique, lop-sided shape would probably have made poor service for an axe for heavy work. Considering the poor finish and the general absence of working one comes to speculate whether the object could be an unfinished axe of the Faardrup shaft hole type. The finish would have required plane grinding of the faces and subsequent engraving of the geometric patterns.

No. 9. B 3971. High-flanged axe. Unknown location, Denmark. About 1500 B.C. Weight: 214 g. Figs. 63–68. Table 10.

The axe has the dimensions 120 × (20–48) × 10 mm. The flanges are wide and somewhat irregular in width and thickness, figs. 63–65, due to substantial deformation by working. They reach widths of 17–18 mm. The butt appears unfinished and terminates in a rough break. In the middle of the axe a moderate stop-ridge appears, clearly a feature modelled in the mould. The edge has been sharpened for the outermost 13 mm, apparently by a combination of cold-working and grinding.

Analytically the axe belongs in the Faardmet group (Liversage & Liversage 1989), being a full tin bronze with substantial impurities of sulphur, nickel, arsenic, antimony, and lead.

Polished sections display a yellow alloy with numerous small (3–15 μm across), blue sulphides, containing a little iron (about 0.1%). The sulphides cover about 1.0% by area. They are deformed to narrow, long veinlets in the cutting-edge and in the exterior 5 mm of the flanges, indicating very heavy deformation. This does not necessarily indicate hot work, since we have shown with our experimental sulphidic alloys, that the sulphides are sufficiently ductile to follow the metal also under heavy coldworking. The axe is pretty solid, displaying only a few micropores up to 100 μm across. No micropores remain in the heavily worked edge and flanges.

Etched sections show a rather homogeneous, recrystallized tin bronze. Almost all δ-phase and coring have disappeared, apparently due to repeated working and annealing. The recrystallized, twinned grains of the interior are 50–100 μm in diameter, and the hardness is 75 ± 3. In the edge and under the flanges the grain size gradually decreases to 10–20 μm, and the hardness increases to 200 ± 5. In these ultra-hard parts the recrystallized grains have visible traces of severe cold-work, such as numerous crossing slipband systems and elongation of grains near the surface, fig. 66.

The general corrosion development is the normal one for the Danish environment. An interior greenish patina covers the axe irregularly as up to 100 μm thick layers, filling micropits, 50–100 μm across with botryoidal, green patina. On top of this is a somewhat thicker gray layer, which is rusty-red in crossed polars, and very irregular.

On this axe destannification is particularly well-devel-

Table 10

	Sn	S	Fe	Ni	Zn	As	Ag	Sb	Pb	Cu	Vol.% Sulph.	Vol.% Lead
J.1968; no. 8516	7.4	–	tr.	0.47	–	0.87	0.06	0.23	0.59	–	–	–
This work	8.0	0.25	0.05	0.49	<0.05	>0.3	<0.1	0.28	0.5	(89.5)	1.0	0.4

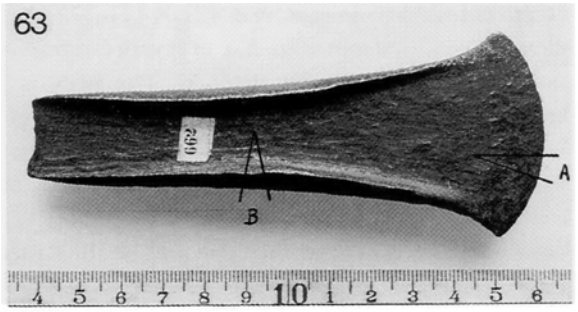

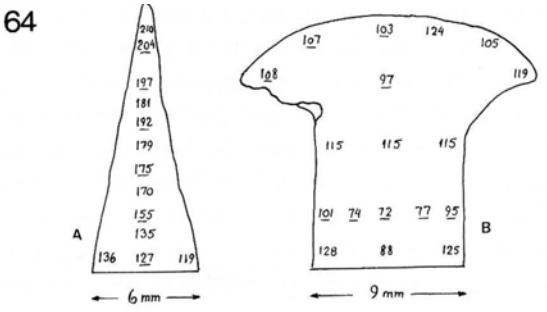

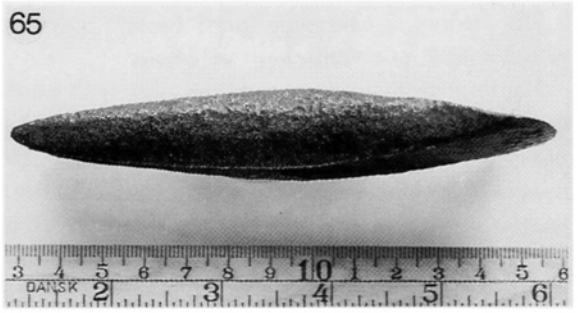

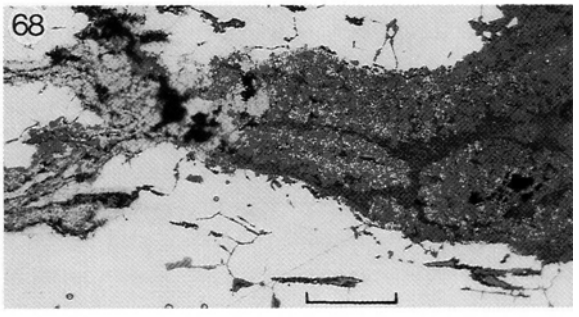

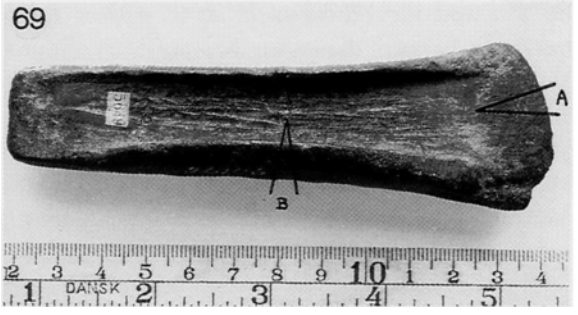

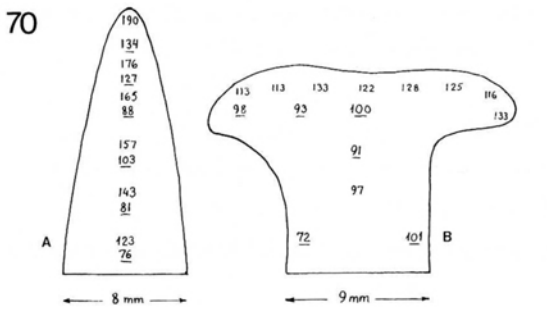

Figs. 63–70. Fig. 63. *No. 9. B3971.* High-flanged axe. 214 g. Fig. 64. Vickers (5 kg) and Microvickers (100 g) hardness af A and B. Fig. 65. The axe seen from above, the edge to the right. Fig. 66. Severely deformed edge with elongated coring due to hammering. Scale bar 0.3 mm. Fig. 67. Almost homogenized material with recrystallized α-grains and sulphides, from the interior. Scale bar 50 μm. Fig. 68. Corrosion pit. The fine, 1–2 μm, white spots in the corrosion products are copper particles from destannification. Scale bar 50 μm. Fig. 69. *No. 10. 26106.* High-flanged axe. 225 g. Fig. 70. Vickers (5 kg) and Microvickers (100 g) hardness of A and B.

oped. At the transition between flange and bulk is a 1 mm deep groove, figs. 64, 68. In this re-entrant part of the axe some "sand" from the casting mould has remained embedded in the surface material and on long exposure in the soil given easy access for moisture. The result is that tin has been selectively removed to form tin-enriched corrosion products while copper has been redeposited as a spongy mass, displaying grains 1–2 μm across. The "sand" particles are still firmly embedded in the corrosion products, on top of which the usual green and grey oxides/hydroxides are found.

SEM-EDAX on the corrosion products confirmed the destannification interpretation. The copper particles are re-precipitated tin-free copper, apparently with a little iron (0.5–1 wt.%), while the enveloping oxides are extremely variable. Some parts are tin-enriched to Cu-Sn ratios of 3 instead of 11 as in the alloy, some are copper-enriched to Cu-Sn ratios above 100, and all contain iron in varying quantities. In addition chlorine, calcium, and phosphorus are common minor impurities in the corrosion products. The surprisingly high iron content, often exceeding the copper content, must derive from the surrounding soil, as do the chlorine, calcium, and phosphorus.

B 3971 is an axe which has been subjected to heavy work, probably a combination of hot- and cold-work, so that the flanges could be raised as much as we now see. The severe deformation and the repeated annealing have removed all coring, dissolved all δ-phase, and closed a majority of the micropores. The grain size is fine, finest in the cold-worked cutting-edge, which reaches a hardness above 200. The axe provides a very fine example of the phenomenon of destannification, which otherwise has received little attention (Tylecote 1979).

No. 10. 26106. High-flanged axe. Badstrup, Uggeløse Sogn, Lynge Herred, Frederiksborg Amt. About 1500 B.C. Weight: 225 g. Figs. 69–74. Table 11.

This is a rather rough and clumsy looking tool (Aner & Kersten 1973,57). It measures 121 × (21–37) 11 mm. Its flanges are 17–20 mm wide due to severe hammering, and the cutting-edge is badly notched. The body is for unknown reasons heavily striated/grooved parallel to the long axis of the tool. Perhaps it is impressions of the mould, perhaps it is from severe scraping in order to remove moulding sand? The 2–3 cm nearest the edge have been hammered both *on* the edge and on the flanges near the edge. This has produced shallow, triangular depressions on the narrow sides near the corners of the blade.

Analytically the axe is a little difficult to rubricate and has according to Liversage (pers. comm.) a deviant composition with unusually high antimony.

Polished sections show a yellow alloy with pin-holes in the interior. Many pin-holes are almost spherical, 0.1–0.2 mm across, others are interdendritic. They are often coated with blue sulphides, and many have during the long exposure in the soil become filled with corrosion products. The sulphides are palmate-lobate and attain dimensions of 30 μm from tip to tip. More normal are 3–10 μm blebs, all in all covering about 5.5% by area. The sulphides are blue, isotropic and of the digenite type, Cu_9S_5, with a little (0.1–0.3%) iron in solid solution.

In the edge and under the flanges to a depth of 4–5 mm the micropores have been closed and the sulphides severely deformed. They are typically stretched to narrow bands and filaments, e.g. 60 × 6 μm or 100 × 2 μm. They are not extensively broken but only plastically deformed, figs. 73–74.

The etched sections show a cored structure on which is superimposed a recrystallized, twinned structure. No δ-phase was identified. In the interior the grain size is about 80 μm and the hardness 79 ± 8, with a pretty large variation because the coring has not been eliminated. In the cutting-edge the grain-size decreases to 10–20 μm and the hardness increases to 134. Under the flanges the twinned, recrystallized grains are 20–40 μm across and the hardness increases to 100. On the whole there are few indications of final cold-work, so it appears that the present medium hardness level is due to repeated cold-work

Table 11

	Sn	S	Fe	Ni	Zn	As	Ag	Sb	Pb	Cu	Vol.% Sulph.	Vol.% Lead
J.1968; no. 8289	5.5	–	tr.	0.21	0	0.73	0.04	2.6	tr.	–	–	–
This work	6.0	1.1	<0.05	0.15	<0.05	>0.3	0.07	1.9	<0.1	(90.0)	5.5	0

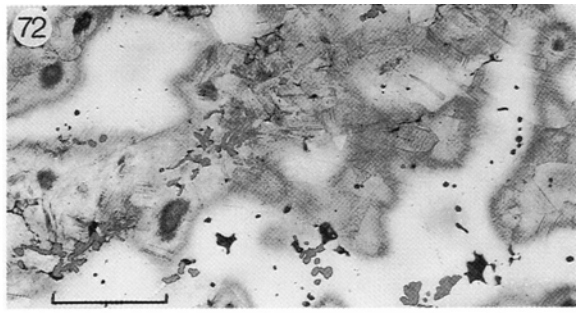

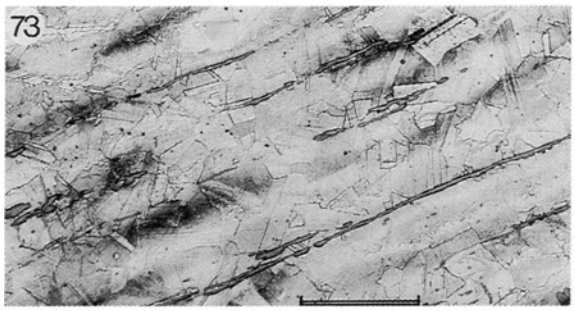

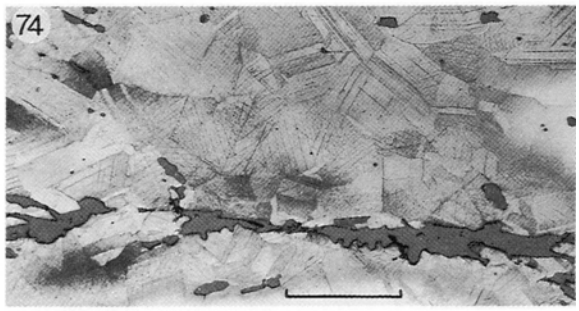

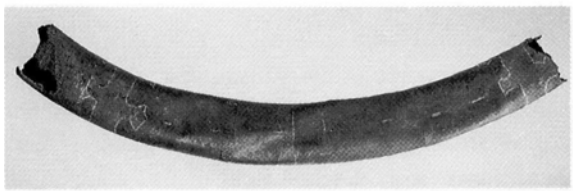

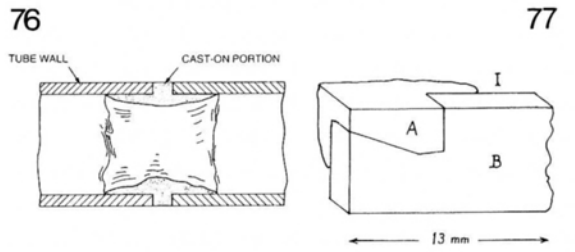

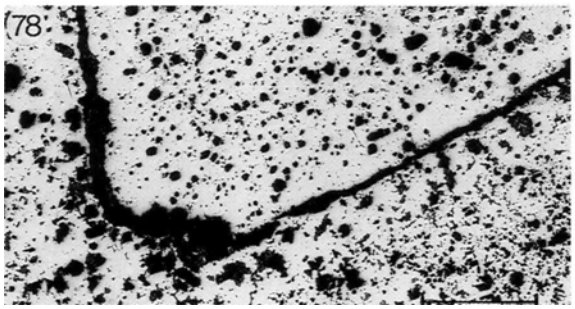

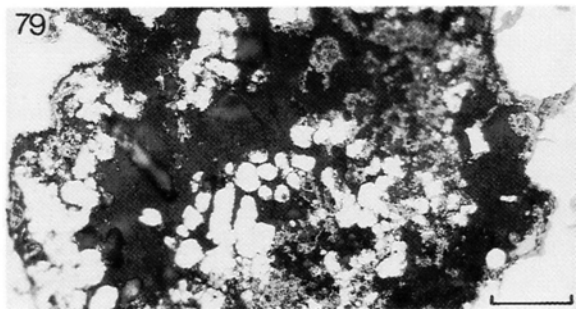

Figs. 71–79. Fig. 71. *No. 10. 26106*. The irregular flanges on the axe. The edge to the right. Fig. 72. Unequilibrated, slightly deformed interior with slip-lines in recrystallized α-grains. Palmate Cu_2S. Scale bar 0.1 mm. Fig. 73. Severely deformed sulphide crystals under the flange, B. Recrystallized grains with slip-lines. Scale bar 0.1 mm. Fig. 74. Detail of severely deformed, but unbroken sulphides, proving their ductility. Slip-lines in recrystallized α-grains. Scale bar 50 µm. Fig. 75. *No. 11. B 15505*. The Hallenslev Lur (from Hallenslev Sogn, Løve Herred, Holbæk Amt). Fig. 76. Reconstruction of the method for joining two tube parts (Holmes 1986:114). Fig 77. Sketch of the joining of tube B with cast-on A metal, compare Fig. 75–76. Fig. 78. The junction between A (top) and B (bottom) was never perfect. Note the numerous pin-holes from casting. Scale bar 0.5 mm. Fig. 79. Destannification of part B. Numerous micron-sized blebs of almost pure copper have been redeposited in voids. Scale bar 50 µm.

and annealing, and that the final process was a mild reheating that did not lead to equilibration.

The general patina consists of an inner 50–200 μm thick "red Cu_2O" layer, and an outer 50–200 μm thick green layer with botryoidal growth. The copper sulphides survive for a while in the corrosion products.

This chisel-like axe stands in shape and composition somewhat apart from the others examined here. It is a sulphide-rich tin bronze with heavy deformation-work on the flanges. The final treatment from the smith was a mild annealing.

No. 11. B 15505C. The Hallenslev Lur. Hallenslev Sogn, Løve Herred, Holbæk Amt. About 1100–900 B.C. Figs. 75–79. Table 12.

The Hallenslev lur was found in 1961–1962 in several fragments and was thoroughly described by Broholm (1962). Broholm paired it typologically with the four lur finds from Maltbæk, Lommelev, Nyrup, and Dauding, placing them in period IV of the Danish Bronze Age, or about 1100–900 B.C. Recently a fragment has been examined by X-ray fluorescence analysis (Gottlieb 1987), yielding qualitative information about the chemical composition. The small sample, which has here been examined by the kind co-operation of Poul Otto Nielsen, Jørgen Jensen, and Birthe Gottlieb, was carefully hacksawed from the lower part of the tube, figs. 6–7 in Broholm 1962. This tube is 1.2–1.5 mm thick, 50 mm in diameter, 50 mm long and weighs 702 g (fig. 75).

The specimen was cut so as to include both a part of the tube length (B) and a part of the meander-connection (A), figs. 76–77. When the lur was originally assembled two tubes, B and C, were cut to a meander shape and positioned firmly about 20 mm apart. Then a mould was constructed à cire perdu so that an annular connecting link, A, could be cast. The liquid metal flowed into the meander-cuts and also added about 1 mm of thickness on the interior of the tube. This reinforcement in thickness and the mechanical interlocking served well to fasten the tube parts securely. It has earlier been assumed that there also was metal-to-metal bonding from remelting the edges, but, as will be discussed below, this appears not to have been the case. The assembly was, however, strong and the later fragmentation of the lur happened outside the assembly regions.

The tube, B.

Analytically, the tube is a low-tin bronze with significant impurities of arsenic, antimony, and nickel. It somewhat resembles axe No. 4 of the Singen group, but the lur is very low in silver, and the two objects are separated in time by approximately 800 years.

The polished section shows a reddish-yellow alloy with a number of interdendritic micropores from casting, fig. 78. Sulphides occur as 5–15 μm blue subangular blebs, that are dead black in crossed Nicols. Many of the interdendritic cavities are filled with material of the same blue colour, but those that are *red* under crossed Nicols can be shown to be copper oxides produced by corrosion. In many of these pockets, and in the copper oxides on the surface, are numerous 1–2 μm copper blebs or up to 10 μm long copper filaments, all the result of corrosive destannification, fig. 79.

The etched section shows a cored casting with a dendrite armspacing of 30–40 μm. The coring is somewhat annealed, probably from reheating associated with casting of the assembly part A. No δ-phase is present, in accordance with the low total of tin, arsenic, and antimony. The hardness is 62 ± 4, in agreement with the annealed condition of a copper alloy low in alloying elements.

The annular assembly part, A.

Analytically, the alloy cannot be classified with the Faardmet group or any other of the groups proposed by Liversage & Liversage (1989), than which it is considerably younger. It differs from the alloy of the tube in its significantly higher tin, arsenic, and sulphur content. It appears that the smith purposefully has added these to

Table 12

	Sn	S	Fe	Ni	Zn	As	Ag	Sb	Pb	Cu	Vol.% Sulph.	Vol.% Lead
Assembly, A	4.0	0.4	<0.1	0.70	<0.05	(1.2)	<0.05	1.4	<0.1	(92.2)	2.0	0
Tube, B	2.4	0.1	<0.1	0.47	<0.05	0.8	<0.1	1.5	<0.1	(94.5)	0.5	0

the tube alloy base in order to create a lower-melting, free-running alloy, which would be well suited for the assembly process. The solidus line of alloy A may have been about 75 °C lower than that of B.

The polished section shows a reddish-yellow alloy, which cannot be distinguished from the colour of tube B. The material is unusually rich in interdendritic microporosities, so much so that a normal hardness determination at 5 kg load, giving the low range of 43 to 49, is misleading. Instead the hardness has been estimated by microhardness determination at 100 g load in massive material to 74 ± 5.

Sulphides are abundant, as 6 × 4, 15 × 5, or 3 μm subangular blebs, adding up to about 2.0 vol.%. In the boundary between A and B, a thin (2–3 μm), continuous Cu_2S layer has formed on solidification, i.e. there has never been established a solid metal-to-metal contact. On the other hand, the geometry of the assembly has served to anchor the two parts securely. The reason for the formation of the Cu_2S layer is, in somewhat simplified terms, that the sulphide nucleates and grows on the colder surface, i.e. the tube B, while the metal phase (copper enriched in tin, arsenic, and nickel) has a lower solidification range and therefore for a short while remains liquid. In addition, the tube B must at the time of pouring the A-metal have been covered by thin copper oxide coatings due to preheating of the mould assembly. This coating would assist in the nucleation of copper sulphide. In short, the finished assembly, although mechanically perfect, never acquired a remelted metal-to-metal bonding.

The etched section shows a cored alloy with sulphides, and a small amount (< 1 vol.%) of δ-phase, occurring as 3–6 μm blebs. The dendrite armspacing is about 30 μm, and the structure is unannealed. There are no indications of hammering or other forms of mechanical working, in contrast to the conclusion reached by Gottlieb (1987,193).

The minute δ-phase areas are located where the last melt solidified on casting. Since this was enriched in low-melting components we find these highly concentrated here. For example, one complex 10 μm area consisted of a lead nodule of which 25% was bismuth, associated with an area with 62% Cu, 20% Sb, 14% Sn, 3% Ni, and 1% As. Although bismuth is certainly present, it is a curiosity and cannot be traced in the bulk analysis.

Corrosion has attacked both parts. Especially the tube, B, has suffered, being covered by an interior, 20 μm thick copper oxide layer (red in crossed Nicols) and an exterior brownish-greenish layer, also very thin, 10–20 μm. The interdendritic cavities and the join between A and B are filled with copper oxides; some feldspar grains ($KAlSi_3O_8$) from the ancient moulding material may be found embedded here. Destannification, in the form of irregular 1–5 μm copper grains, is only observed in the Cu_2O of the B part. It is not obvious, why the very similar, but more tin-rich A-alloy has not suffered destannification.

The lur has been cast by the cire-perdu technique as described by Broholm (1962), and individual tube parts have been assembled by casting on annular rings. This was done in one step; no signs of the two-step operation suggested by Gottlieb (1987, fig. 5) could be detected. All the metal of A, fig. 76, is coherent and of the same composition. No parts of the examined specimens have been worked after casting.

No. 12. B 17482. The Ulvkær Lur No. 2. Near Tornby, Horne Sogn, Vennebjerg Herred, Hjørring Amt. About 700 B.C. Figs. 80–86. Table 13.

Fragments of a lur were found in August 1988 by Orla Pedersen at Ulvkær, near Tornby, Vendsyssel (Lysdahl 1988, 1989). Further fieldwork revealed more fragments, and these could finally be restored as a pair of lurs, the first ever found in Vendsyssel. The instruments had been lying in a 3 m thick turf deposit overlain by blown sand, but the exact conditions will never be known, as the turf with the lurs had been removed in bulk during mechanical earth moving operations. The best preserved of the two lurs (No. 1) weighed almost 3 kg and measured 175 cm along the curved tube, fig. 80.

The material here examined is a 1.8 g fragment which comes from lur No. 2; it was not so well preserved, having been somewhat molested by a bulldozer. The fragment is from the inner part of the circular end-plate, which had broken along corroded, dendritic grain boundaries. The thickness of the plate now varies from 0.7 to 1.0 mm. Apparently the original thickness was about 1.0 mm while the present thinner parts mainly are due to general corrosion, fig. 81.

The surface is covered with black to blue and greenish-black corrosion products which in places are blistery. Below the 50–100 μm thick outer crust is a 50–100 μm, irregular, moss green patina which in most places is in direct contact with the dendritic metal.

The corroded fragment was broken in three pieces and mounted in coldsetting resin so as to show both a full cross-section and a view of the surface itself.

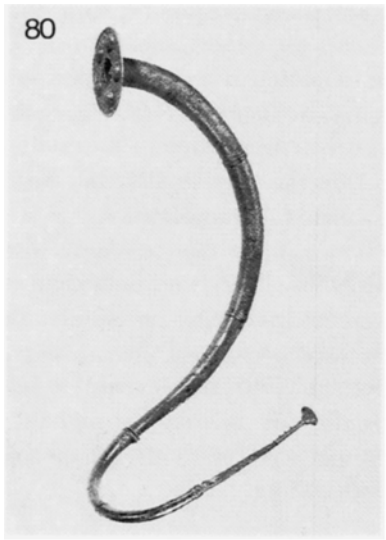

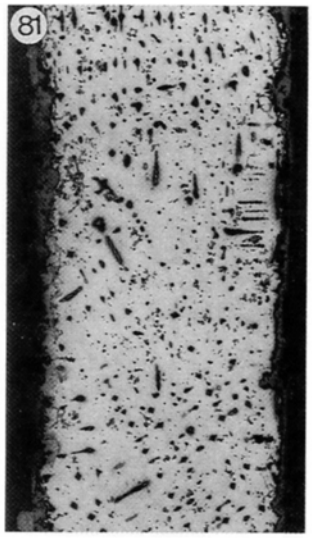

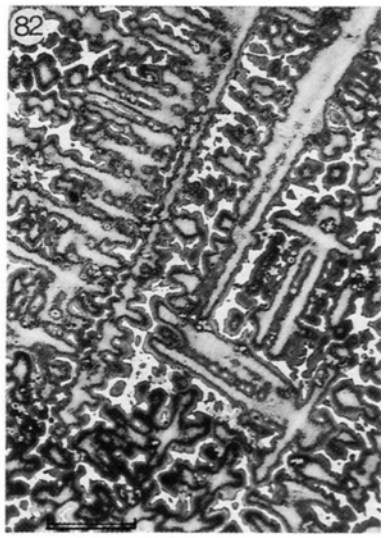

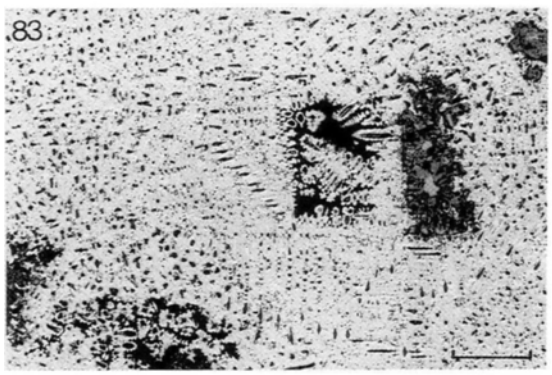

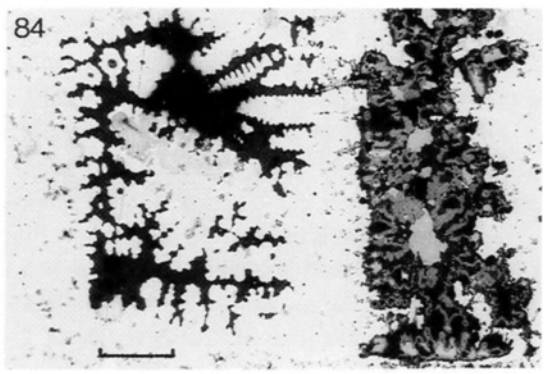

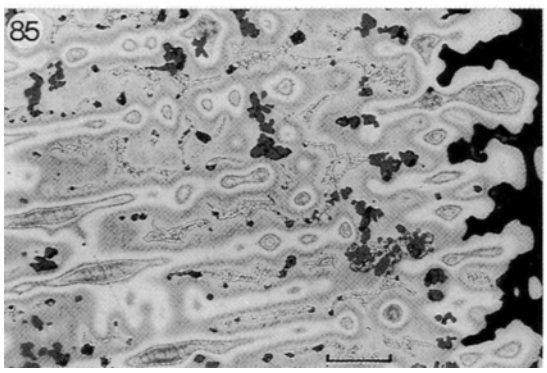

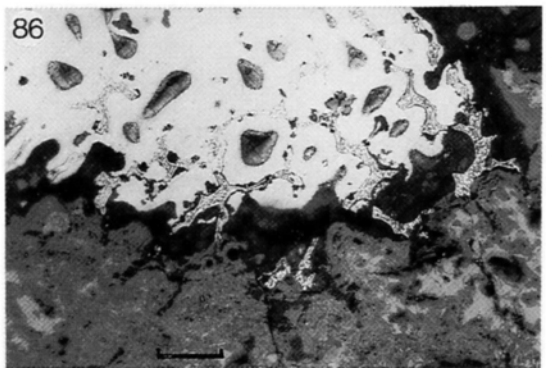

Figs. 80–86. Fig 80. *No. 12. B 17482*. The Ulvkær Lur No. 1. (Courtesy Nationalmuseet). Fig. 81. Full cross-section of a 1.0 mm thick fragment, broken from the circular end-plate of the Ulvkær Lur No. 2. Fig. 82. Cast, dendritic high-tin bronze with significant δ-phase. Scale bar 0.1 mm. Fig. 83. Because the lur was cast and never subsequently worked, all micropores are still well-defined voids. The void on the right is now partly filled with corrosion products. Scale bar 0.5 mm. Fig. 84. Detail of Fig. 83: Dendrites radiate into voids. Scale bar 0.2 mm. Fig. 85. Detail of Fig. 84: Cored α-phase, extensive δ-areas, and globular-palmate copper sulphides. Scale bar 50 μm. Fig. 86. Corroded surface. The α-phase adjacent to δ is the first to be attacked. The location of the δ-phase is still visible in the black corrosion products. Scale bar 50 μm.

Table 13											Vol.%	
	Sn	S	Fe	Ni	Zn	As	Ag	Sb	Pb	Cu	Sulph.	Lead
This work	13.1	1.0	0.10	0.11	<0.05	0.5	<0.1	<0.1	3.0	(82.1)	5.0	2.5

Analytically, the lur is a high-tin bronze, rich in lead and sulphur. Its composition is entirely different from that of the Hallenslev Lur, and it is the object with the most tin of any examined in this study. In addition to the elements reported below, we found 0.25% Co. Ni and Co were enriched in the δ-phase relative to the α-phase by factors of respectively 3 and 1.5.

Polished sections show a yellow, cast alloy with many microporosities. The blue sulphides are conspicuous as blebs or palmate inclusions, 5–20 μm across, constituting about 5 vol.%. The micropores are interdendritic empty voids, or are filled with complex corrosion products, figs. 83–84.

Etched sections show a beautiful cored casting with substantial amounts, about 20 vol.%, of bluish-grey δ-phase, fig. 82. Lead occurs as 3-25 μm rounded blebs associated with the δ-phase and the sulphides. The morphology of the δ-phase, the sulphides, and the lead all show the object was neither hot nor cold-worked after casting and was not reheated for annealing. The hardness is 120 ± 12, displaying a rather large spread due to segregation and microporosities. SEM-EDAX work on the individual phases showed that the copper sulphide was as usual of the Cu_2S-type and had from 1.2 to 3.6 wt.% Fe in solid solution. The iron content of the adjacent metal phase is below the detection limit of 0.05 wt.%.

The lead segregates are pure lead and do not display the dirty appearance of the A-part of the Hallenslev lur. The δ-phase is similarly a rather pure phase, primarily consisting of $Cu_{31}Sn_8$, in which are minor impurities of arsenic (about 0.4%), nickel (about 0.2%) and cobalt (about 0.16%), fig. 85.

The corrosion products are complex grey-blue (black in crossed Nicols) and black (black in crossed Nicols) layers, often developed in botryoidal forms. Nearest the metal are discontinuous greenish films, that are green in crossed Nicols. The copper part of the δ-areas and the copper zone around the sulphides are the first to be attacked by the corrosion. No simple, red copper oxides and no destannification was observed. The cohesion of the lur is weakened considerably by the interdendritic corrosion, fig. 86.

A preliminary examination of the corrosion products showed that they are extremely variable, with Cu-Sn ratios varying from 0.7 to 2, compared with 6 for the bulk alloy, and with significant amounts of iron, sulphur, phosphorus, silicon, and chlorine, introduced from the adjacent soil and peat. Some of the corrosion products are similar in structure and composition to those reported on axe No. 7 (B 4077) which was also found in peat.

The Ulvkær lur is the youngest of our bronze objects and represents a new alloy type which is rich in tin, lead, and sulphur, and poor in nickel and antimony. Cobalt is present at the low level of 0.25%. The casting succeeded very well, and no further hammering or annealing has taken place on this part of the lur, which is the circular end-plate.

DISCUSSION

The analytical data.

Ten of the twelve objects have already been analyzed by the spectrographic method (Junghans et al. 1968). Inspection shows that the material for spectrography was obtained by drilling 1 mm holes, generally in the middle of the axes. Presumably the drillings from the outermost, corroded layers were discarded before analyzing. However our metallographic studies have shown that many of these ancient objects are rich in corrosion products also in the interior, especially along grain boundaries and in interdendritic micropores that originated during casting. Much of the corrosion is selective, removing either copper, tin, or arsenic, depending on alloy type and environment, so the presence of corrosion products in the drillings may have influenced the results.

Nevertheless, the differences between our results and Junghans et al's spectrographic data are small. In general, our values for iron, nickel, silver, antimony, zinc, and lead agree very well with the old data sets, and so do our tin values for low-tin alloys. For the full tin bronzes there are small discrepancies, but we believe our tin data to be the better, because they are well supported by the metallographic structure. With respect to arsenic the

spectrographic data are apparently better than ours, mainly because our instrument has difficulty in the quantitative separation of the As K_α line (10,530 eV) from the Pb L_α line (10,550 eV).

With respect to bismuth, cobalt, and gold, which were reported as nil in the spectrographic data sets, we can support this by stating that they are certainly below 0.05% in the bulk samples, and were not detected either as discrete blebs or as inclusions when searched for under the scanning electron microscope. However, traces of bismuth were found in lur No. 11, and traces of cobalt in lur No. 12.

Sulphur is an important element, which cannot be measured by the spectrographic method. On the other hand it is easily detected by metallographic examination, when it appears as blue sulphides which are dead black in crossed Nicols and have the general composition, Cu_2S. The bulk sulphur value may then be calculated using planimetry, as we have done here in the last columns of the analytical tables. Also sulphur is easily detected and measured using SEM-EDAX equipment, and the two results generally agree very well. When discrepancies occurred we preferred the planimetric results because the instrument had problems with separating the signals from S K_α (2.307 eV) and Pb M_α (2.342 eV), generally leading to too high sulphur concentrations. These conclusions were supported by analyzing synthetic series of copper-tin-lead-sulphur alloys.

Turning now to the composition of the ancient objects several interesting points are revealed by inspection of table 14.

First, the two oldest objects are almost pure copper-arsenic alloys. No sulphur is present; instead a host of copper oxide and copper-lead arsenate inclusions are found, proving that the two axes were produced by casting and not, for example, by hammering some native copper. That native copper can be excluded as a source of metal is supported by the observations of Maddin et al. (1980) and Matteoli & Storti (1982) who find that native copper is extremely pure, similar to or better than modern electrolytic copper for electric cables. We therefore conclude that the axes have been produced by smelting of oxidised minerals from the gossan. Minerals in question could be cuprite (Cu_2O), malachite ($Cu_2(OH)_2CO_3$), azurite ($Cu_3(OH,CO_3)_2$), brochantite ($Cu_4(OH)_6SO_4$), atacamite ($Cu_2(OH)_3Cl$), and antlerite ($Cu_3(OH)_4SO_4$). Since the last three are characteristic of weathering under arid conditions, such as in the Chilean Atacama Desert, it is probable that the ores with which we are concerned were a mixture of the first three, possibly with cuprite as the dominant mineral. Arsenic, antimony, and lead are usually enriched in the gossan as oxides, carbonates, and sulphates and must have been included in small proportions in the ore. Also a number of copper arsenates are known from the gossan, for example olivenite ($Cu_2(OH, AsO_4)$), cornwallite ($Cu_5[(OH)_2AsO_4]_2$), clinoclase (Cu_3

Object		Sn	S	Fe	Ni	As	Ag	Sb	Pb	Cu*	Hardness range HV5	Approx. date B.C.
1	B2926	<0.1	<0.1	<0.05	<0.05	1.4	<0.1	<0.1	<0.1	98.4	66– 97	3500
2	B5556	<0.1	<0.1	<0.1	<0.05	0.47	<0.1	<0.1	<0.1	99.3	57– 81	3500
3	B1094	<0.1	0.11	<0.05	0.08	0.50	0.9	0.4	<0.1	97.8	53– 91	2000
4	11073	2.1	0.15	<0.05	0.74	0.36	0.7	0.8	<0.1	95.0	69–161	2000
5	26073	8.8	0.35	0.08	0.37	ca.1	0.09	0.22	<0.1	89.5	85–201	1700
6	21075	8.8	0.15	<0.05	0.74	ca.1	0.22	0.5	<0.1	88.5	91–257	1800
7	B4077	9.4	0.40	<0.05	0.37	ca.1	<0.1	0.18	0.9	88.0	76–165	1700
8	B5564	8.4	0.23	0.12	0.46	ca.1	0.16	0.28	1.2	88.2	91–155	1700
9	B3971	8.0	0.25	0.05	0.49	ca.0.8	<0.1	0.28	0.5	89.5	72–204	1500
10	26106	6.0	1.1	<0.05	0.15	ca.0.7	0.07	1.9	<0.1	90.0	72–134	1500
11A	B15505A	4.0	0.4	<0.1	0.70	1.2	<0.05	1.4	<0.1	92.2	70– 78+	1000
11B	B15505B	2.4	0.1	<0.1	0.47	0.8	<0.1	1.5	<0.1	94.5	58– 66	1000
12	B17482	13.1	1.0	0.10	0.11°	0.5	<0.1	<0.1	3.0	82.1	106–134	700

* estimated

\+ estimated from the hardness at 100 g load

° in addition 0.25% Co

Table 14. Composition and hardness of ten axes and two lurs (the three last lines). Zinc, cobalt, bismuth, and gold searched for, but present at levels below 0.05%, except for no. 12, see the text.

$(OH)_3AsO_4$), cornubite ($Cu_5[(OH)_2AsO_4]_2$), euchroite ($Cu_2(OH, AsO_4)$, $3H_2O$), and tirolite ($Ca_2Cu_9[(OH)_{10}(AsO_4)_4]$, $10H_2O$) (Ramdohr & Strunz 1967; Strunz 1970). It is not known to what extent the natural minerals at this ancient date were sorted before smelting, but we believe that it would have been possible even then to mix them to give a specific alloy if the desire were there. Charles (1985) has some interesting viewpoints on this early development.

The two old axes were probably cast in Central Europe, the present Austria-Hungary, exported to Denmark and never remelted, for reasons given p. 76. Analytically, they belong in the Bygmet group, which comprises many other early flat axes (Liversage & Liversage 1989).

The next two axes are typologically younger and represent analytically a significant change since a number of other elements are now present, first of all sulphur. In our opinion the presence of sulphur reflects the first utilization of sulphidic copper ores. In Central Europe there is a host of these ores, ranging from simple copper sulphides (chalcosite, covellite) to complex ones containing also arsenic (e.g. enargite), antimony (e.g. tetrahedrite), iron (e.g. chalcopyrite), silver (e.g. stromeyerite), bismuth (e.g. emplektite), and the very complex ones, containing both iron and tin (e.g. stannite), both lead and antimony (e.g. bournonite), or silver, arsenic, antimony, iron, zinc, and tin together (the Fahlerze).

Nickel does not occur as a component of complex copper hydroxides or sulphides, but it may be present mixed with the other minerals as arsenides (e.g. niccolite, NiAs), antimonides (e.g. breithauptite, NiSb) or complex sulphides (e.g. pentlandite $(Fe,Ni)_9S_8$). The thorough examination of an early Bronze Age hoard of copper ingots from Obereching at Salzach, North of Salzburg, demonstrated that the Austrian mixed ores could produce a semifabricate which was rather variable, but generally rich in nickel, sulphur, iron, arsenic, and silver (Moosleitner & Moesta 1988). On further processing and remelting, the iron, nickel, and sulphur in particular must have been reduced to the lower values which are known in the finished objects.

When the sulphide ores are roasted and smelted part of the impurities (arsenic, antimony, nickel, iron, silver, sulphur, lead) follows the copper metal, while another part is removed as volatiles or is eliminated in the slag. The partition coefficients may be known for individual components under laboratory conditions, but it is almost impossible to predict the result of smelting complex ores under the rather unknown conditions of ancient times. Tylecote (1980) has reported some valuable observations on the experimental smelting of nine different ores; he studied the effect of fluxing and the distribution of main impurities after melting under oxidizing or reducing conditions. He found that most of the iron and other impurities can be reduced in amount by controlled remelting in a crucible, and that the degree of refining will depend on the time and care given to the refining operation. Much discussion has revolved around these early smelting processes, and the interested reader should consult, e.g. Percy (1861), Tylecote (1976), Jovanovic (1980), Moesta et al. (1984), Hauptmann (1985), and Riederer (1987) and references therein.

The situation is very complex. Suffice it to say that the analytical evidence from the present examination seems able to show groups of objects that were produced from similar ores by similar methods during distinct periods, and the groups were to some extent related to the groupings proposed by Liversage & Liversage (1989).

Thus axe No. 3 would have been smelted from an ore type from which tin is absent (Ösenring composition), while No. 4 would have been smelted from a different ore type (Singen composition) contaminated by one or more tinminerals such as stannite (Cu_2FeSnS_4) or cassiterite (SnO_2). Such mineral associations are known to occur in Saxony, Bohemia, and Austria, or generally speaking in the Fichtelgebirge and the Erzgebirge. It is unlikely that copper occurrences in Sweden, Norway, or Finland, although rich today, were exploited in the Bronze Age. Similarly the Helgoland copper occurrence has another fingerprint with respect to the associated elements (Schulz 1984) and can hardly be associated with these tools. The axe No. 4 is apparently from a period when separate tin ores were first being used. Otherwise it would be difficult to understand graph 9 in Liversage & Liversage (1989), where 78% of all objects have tin contents less than 2%, while the remainder show variable additions, deliberate we take it, of up to and over 10%.

The next six axes, Nos. 5–10, are full tin bronzes with 6.0–9.4% Sn. No naturally occurring mineral mixture will by smelting yield such a rich tin bronze. It may be assumed that by this time the craftsman had learned to appreciate the new tin bronze and had a continuous supply of the proper ore or metal. He may even have experienced the toxicity associated with the smelting of copper-arsenic alloys and alone for this reason preferred the copper-tin alloy. However arsenic followed him for a long

time, as witnessed by this suite of ten axes. Charles (1985) in an interesting paper discusses the sequential steps from copper-arsenic to copper-tin bronzes and speculates that Hephaistos, the only Greek god who was imperfect, acquired his lame leg from arsenic poisoning.

By judicious mixing of tin or tin ore with the copper alloy in fixed ratios the smith could obtain a full tin bronze with the desired properties. An addition of metallic tin is apparently the simplest way to make the new alloy, since tin melts at 232 °C and will start coating and diffusion into the copper long before this has melted. Since, however, we rarely if ever find the raw tin on archaeological smelting sites, it is speculated that the alloying material was cassiterite, SnO_2, which when heated under charcoal with a molten copper alloy will be reduced to metallic tin and enter the alloy to form the desired bronze. From the high sulphur content of the finished objects we conclude that the copper ores were for a major part sulphidic, and they still carried some arsenic.

While copper ores are widespread, it has long been a problem where the tin ores came from. It is certain that cassiterite from Cornwall and Devon was used as early as 2200 B.C. for the production of early British bronze axes (McKerrell 1978), and it is also plausible that the extent of the Cornish deposits was sufficient to cover all the needs of civilization from the beginning of the full Bronze Age onwards; but whether this was actually done is another matter (Tylecote 1978). Small deposits are known to have existed in the Erzgebirge, for example at Zinnwald, and in Bohemia at Schlackenwald (Riederer 1987). Very recently, cassiterite deposits and ancient mines have been documented at Bolkardag in Anatolia (Yener & Özbal 1987; Yener et al. 1989) from where the tin ores may have been traded around the Mediterranean Sea and further inland. Possibly the tin ores reached the smelter as concentrates of tin-rich minerals, perhaps as mineral sand. This material is rather inconspicuous and may have been overlooked when excavating ancient smelting sites (Charles 1985). However, it is equally possible that tin at an early date was traded in the shape of metal ingots. Thus, an ancient trading ship from about 500 B.C. was recently discovered in the Mediterranean Sea near Haifa, and several brick-shaped tin ingots, each weighing from 11 to 22 kg, were recovered (Rothenberg 1980).

Denmark has absolutely no copper or tin ores and must have received everything from abroad. However it is a mystery in what form the metal was imported, as ingots are almost or entirely unknown. No doubt part of the demand was met by recycling of metal already in the country, but the results presented by Liversage and Liversage (1989) show that the largest factor affecting impurity pattern was import of new metal – especially in the case of the sudden change-over at the beginning of the full Bronze Age (at about 1750 B.C.) to a full tin bronze, usually of Faardmet pattern.

The last two objects are lurs, i.e. musical instruments, cast in the cire perdu technique with a very thin (1–1.5 mm) wall thickness and never subjected to hammer-work. They are substantially younger and the alloy compositions are different from those of the axes with respect to both tin and accessory elements. In No. 12 we meet a tin-lead-sulphur-copper alloy, where the alloying components are at an extremely high level. Arsenic is still present, but the other common accessory elements, nickel, silver, and antimony have almost disappeared. Instead, cobalt for once appears at the low level of 0.25%. The alloy corresponds in many respects to the Etrurian bronzes used for the casting of vessels and statuettes (e.g. Riederer 1987). No doubt the alloy was chosen because well suited for the purpose.

The Hallenslev lur appears to have been made of bronze of two compositions, which were selected with a knowledge of their melting ranges, the one with the lower melting point having been made as a "solder" to join the tubes. That this did not succeed in terms of metal-to-metal bonding, but only in terms of mechanical interlocking, was probably never realized. The low-tin alloys have resulted in relatively poor castings with very many internal holes and interdendritic microporosities.

A final point concerning the analyses: our twelve objects are low in iron. We shall see (paper in preparation), that Danish bronze objects from the Iron Age and the Viking Age have significantly higher iron content, usually in the range 0.2–0.3%. This may be attributed to other ores, but it may also have been caused by the extensive use of iron in smelting practice, i.e. for ladles and stirring poles. This practice would have introduced significant portions of iron into the copper alloy melt. Apparently most of the iron present in the ancient objects studied here is in solid solution in the copper sulphides.

The structure and the mechanical properties.

Most of the axes have been worked to different degrees after casting. Only the tongue-shaped axe and the shaft-hole axe are still largely in the as-cast state.

It appears that all axes, except the oldest one, were cast in symmetrical bivalve moulds, edge-down. However, the finishing by grinding and hammering has entirely removed all casting flashes and possible indications of the positions of gates and risers. The oldest, tongue-shaped object preserves a ridge which may be interpreted as an impression of a crack in the flat mould in which it was cast.

Copper alloys are even today difficult to cast so that they are entirely solid. Very often voids and microporosities are found and these are generally located were the dimensions change abruptly. However all our axes have more or less the same simple, wedge-shaped form and evenly dispersed voids. The microporosities make the bronze sensitive to bending and breaking strains, so that their transverse strength is significantly decreased. This is demonstrated by the low-flanged axe, No. 3, that has failed in bending, cracking in two places.

Hammering closes the microporosities and improves the mechanical properties of the alloy. The cutting-edges have all been hammered and generally no voids remain for a distance of 10 mm from the edge. The flanges have also been hammered, and the voids have disappeared to a depth of 3–5 mm. Hammering has deformed the sulphide inclusions and they have been altered from their original palmate to subangular shape to irregular filaments. We have shown that the sulphides are sufficiently ductile to deform even under cold-work, so the presence of these elongated inclusions is not alone a valid indication of hot-work.

On cold-working, the hardness and strength increase ever more until maximum values of about 3.5 times that of annealed material are reached. If the desired shape has not yet been reached, a recrystallization anneal can be performed, i.e. the object can be reheated to 600–700° C for anything from 10 minutes to an hour. Thereby the hardness decreases substantially, and the ductility improves so that the object can be shaped further by renewed cold-work. In addition, the coring slowly becomes eliminated by diffusion, and the copper-rich α-phase recrystallizes as equiaxed, twinned grains. The value to us of the sulphide inclusions lies in the fact that on annealing they retain their elongated shapes, and thus document previous deformation, while the metal grains around them recrystallize to equiaxial shapes.

The softest state is reached on repeated working and annealing, ending with slight deformation (10–20 %) followed by a full anneal. Such material has not been identified in this study.

It is instructive to compare the hardness of the lurs, which have been cast and never worked, with the axes, which after casting have been exposed to different combinations of working and annealing, fig. 87. Here the hardness ranges of all objects have been plotted against the composition. The abscissa is the sum of tin, nickel, arsenic, antimony, and silver, which all are known to increase the hardness. This is a rough procedure, but may nevertheless help to explain the phenomena.

The lurs, Nos. 11 A, 11 B, and 12, have the small hardness range appropriate for cast objects. They fall entirely within the band of variability for cast or annealed objects. The tube, No. 11 B, is the softest because it was annealed when preheated during the casting-on of component 11 A. This, and the tube, No. 12, are located in the relatively hard, upper part of the band, because they are thin-walled castings with a high cooling-rate and fine dendritic microstructures.

The axes show a wide range in hardness. Axe No. 6 has as the final production step been cold-worked to a reduction of over 60% on the edge and has not been annealed. The ratio of edge-hardness to bulk-hardness is 2.85, which suggests severe cold-working. Also axes Nos. 4, 5, and 9 have as the final step been heavily cold-worked to reductions of about 40%. The recrystallized grains are elongated and with many internal striations, proving that the final step was cold-working. or perhaps cold-working followed by some mild annealing.

In contrast, axes Nos. 2, 3, 7, and 10 have been severely worked with the purpose of shaping the flanges and edges, and have at one time during production had the high hardnesses corresponding to 50 or 60% reduction. However the final step was an anneal, not very thorough, but sufficient to reduce the hardness substantially.

Finally, objects Nos. 1 and 2, based upon copper and arsenic alone, are surprisingly hard in relation to their composition, whether they are judged by fig. 87 or by fig. 19. Perhaps the long exposure time, over 5000 years, has resulted in the separation of a submicroscopic, arsenic-rich, intermetallic phase, giving rise to age-hardening. For this to occur it is required that the copper-arsenic diagram have a reclining solvus line similar to what is known to exist in the related Cu-P, Cu-Sb, and Cu-Be systems. However, the Cu-As diagram has not been well studied at low temperatures, and the question has so far recieved no attention.

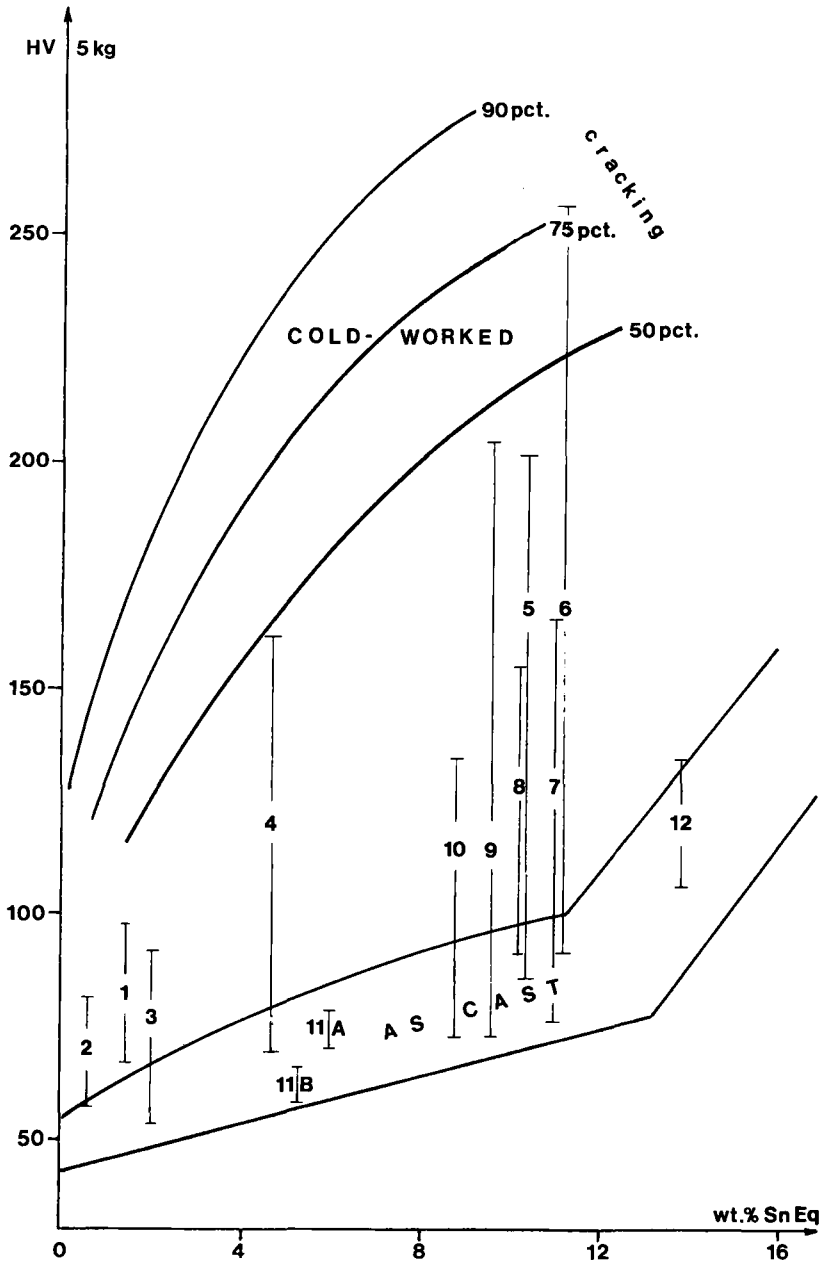

Fig. 87. Vickers hardness (5 kg) of all 12 examined objects superimposed on fig. 1. The abscissa is % Sn Eq., i.e. the sum of Sn, Ni, As, Ag, and Sb. Since the lurs (11, 12) have been finished by casting, their hardness must fall within the lower band. All the other objects show varying combinations of cold-work, hot-work and annealing.

The casting structure, microporosities, and segregation are fully preserved in the lur components, Nos. 11 A, 11 B, and 12. Modern copies of the lurs have been made from rolled brass or tin-bronze, and have completely solid metal walls. In view of the fact that sound waves are significantly attenuated by phase boundaries and particularly by internal voids, it may be speculated that the quality of the sound from a modern replica would be somewhat different from that of the ancient, pore-filled instruments.

Corrosion.

It has not been a purpose of this study to examine the corrosion products, but we have a few observations.

On the copper-arsenic alloys, No. 1 and No. 2, the inner corrosive layer is red copper oxide (Cu_2O), while the outer one is a greenish patina. In contrast, on most of the other objects, which have more alloying elements, the inner layer is a greenish patina, followed by greyish-brownish layers of a complex nature. These layers are significantly depleted in copper content, the copper having been removed in solution.

On axe No. 7 we observed two sulphidic layers of which the exterior layer, 1 mm thick was orthorhombic Cu_2S, while the inner was a complex tin-copper-arsenic sulphide. The axe had lain in anaerobic conditions in a peat bog. A similar, less well-developed layer was detected on the Ulvkær lur, which also was discovered in turf.

Destannification was very well developed on the lur component No. 11 B and on the axes No. 8 and No. 9. The fine, irregular or filamentary copper particles were generally below 10 μm in size. They consist of copper, apparently with up to 1% Fe in solid solution, and are located in red copper oxide. Tylecote (1979) was of the opinion that arsenic inhibits destannification, but our data, on full tin bronzes with about 1 wt.% arsenic, show that arsenic had little effect under the conditions observed.

Grain boundary corrosion is common in those axes which were annealed as a final step, e.g. axe No. 10, while corrosion along slip lines of the cold-worked metal is well developed in axe No. 6, the one which had been severely hammered. The corroded slip line grid is otherwise absent or only present as a minor feature, probably because of the slight annealing to which the other objects had been subjected.

A final observation relates to the microporosities of the cast objects. These were voids, almost under vacuum, immediately after casting, and many of them were interconnected. If open to the surroundings they easily corrode, generally giving rise to red copper oxides. The lur parts Nos. 11 A and 11 B are good examples of this behaviour.

CONCLUSIONS

1. The spectrographic data of Junghans et al. (1968) are supported by our results.
2. The two oldest objects are copper-arsenic alloys, without sulphides. They are interpreted as produced from a sulphide-free gossan in Central Europe, possibly in the present Austria-Hungarian region.
3. The later objects are rich in sulphides and are interpreted as having been produced from a sulphide-containing gossan, or from sulphides proper.
4. The presence of sulphur is very close to a guarantee that an object is ancient and not a 20th century replica. Replicas will have been made from modern alloys, and these are all sulphide-free.
5. Axes Nos. 5–10 and the lurs have tin at levels which suggest a deliberate addition of tin metal or tin ore to obtain specific properties.
6. Even after the introduction of tin arsenic remains present in all the examined objects at levels of 0.4–1.0 wt.%.
7. The objects are poor in zinc, cobalt, gold, and bismuth, i.e. these elements occur at levels below 0.05 wt.%, our equipment's limit of detection. Only the LBA lur No. 12 shows some cobalt, 0.25%.
8. Lead is present in four objects, the axes No. 7, No. 8, and No. 9 from the early Bronze Age and the Ulvkær lur from the late Bronze Age, which has no less than 3.0 wt.% lead.
9. Iron in prehistoric bronzes is very low. Although it has been proposed, based upon the rusty appearance of some corrosion products, that iron might be a significant alloying element, this is not so. When iron is present in very small quantities it is not evenly distributed throughout the metal, but is found in solid solution in the copper sulphide inclusions.
10. Samples taken from different positions show that individual objects are of the same composition everywhere, within analytical error. Inverse segregation was not observed.
11. The tongue-shaped "axe" (No. 1) and the shaft-hole axe (No. 8) are unsymmetrical, unfinished, and made with impure alloys. It is suggested that they represent semi-fabricates.
12. The presence of sulphides (Cu_2S or Cu_9S_5) is helpful, because they preserve evidence of the ore type, tech-

nology (such as the composition of the furnace atmosphere), the solidification by preferential nucleation (No. 11 A), and the degree of working.

13. Eight of the ten axes have been worked on both the cutting-edges and the flanges. Four of them were left in the cold-worked hard condition, four others were annealed to somewhat lower hardnesses.
14. The working of the edges and the flanges served a) to improve the shape, b) to close the microporosities, c) to add substantial hardness.
15. The hardness of the cutting-edge is above 150 on six axes, and above 200 on three of these. The hardness of cold-worked, low-carbon wrought iron is in the same region.
16. The addition of arsenic hardens copper significantly more than the same weight % tin addition. On cold-working the differences become still more pronounced (figs. 19–20). Early Bronze Age axes from Denmark usually contain as little as 0.5–2.0 wt.% As, but they are seen from this point of view legitimate arsenic bronzes.
17. When cold-working these alloys, the hardness increases easily by a factor of 3. Cold-working beyond 70–80 % introduces risks of cracking, ruining the edges or the flanges. A proper anneal before this degree of reduction is reached serves to soften the metal, so that it can be further worked without the risk of cracking. The softest state of any alloy will be reached by thorough annealing after slight reduction (10–20 %).
18. The hardness of complex copper alloys is not simply additive. Nevertheless, in fig. 87 an attempt is presented to display the range of cast, cold-worked, and annealed alloys. Phosphorus which is present in many modern bronzes as a deoxidizing agent and known to add substantially to the hardness, was not present in our synthetic series of alloys.
19. The lurs are unworked. A lower-melting alloy, No. 11 A, has been selected by the ancient smith to prepare the assembly of individual tube segments. The lurs have abundant microporosities and owing to corrosion are much more fragile today than in the Bronze Age.
20. The corrosion products range from simple red copper oxide, Cu_2O, to complex, copper-depleted, greenish, brownish, or blueish oxy-hydroxycarbonates, which were not further examined. Iron and chlorine are common components of the corrosion products and must have been introduced from the environment during the long exposure to ground-water. It is therefore important that no corrosion products should be included in the analysis.
21. Destannification is well-developed on three objects, No. 8, No. 9, and No. 11 B, in spite of the presence of almost 1 wt.% arsenic. The re-precipitated metal is almost pure copper, but apparently has up to 1 wt.% iron in solid solution.
22. The axe No. 7 has lain in an anaerobic, peaty environment and acquired a millimetre-thick covering of Cu_2S and of complex copper sulphides. The sulphur is derived from the environment.
23. Corrosion of annealed alloys is generally intercrystalline. Corrosion of severely cold-worked alloys generally follows the deformation grid of the metallic grains, suggesting stress-corrosion.
24. The chronological arrangement of objects 1–12 was suggested before the start of this project. The analytical data and the structural observations let us vaguely distinguish five groups, more or less overlapping in time: a) Cu-As-O, b) Cu-As-S, c) Cu-As-low Sn-S, d) Cu-As-high Sn-S, and e) Cu-high Sn-S-Pb. This development occurs over about 2800 years in our area, from about 3500 to 700 B.C.
25. The combination of spectrographic analysis and microprobe analysis with scanning electron microscopy and classical metallography, including hardness determination, is the best way to examine ancient bronze objects and their technology.

Vagn F. Buchwald and Peter Leisner, Institute of Metallurgy, *Danmarks Tekniske Højskole*, DK-2800 Lyngby.

Acknowledgments

It is our great pleasure to thank a number of polytechnic students who have shown a deep interest in ancient Danish metallurgy over the years and made many important contributions to its study: Arne Jouttijärvi, Poul Bøjsøe-Jørgensen, Susanne Kaarøe, Leif Andersen, Pernille Dorph, Christian Bøje-Møller, and Henrik A. Larsen. We thank Edith Johannsen, Inger Søndergaard, Annelise Steffensen, Mogens Keller, and Roald Norbach for all the time and care they spent in assisting with the preparation and analysis of the limited amount of sample material. Further, we wish to thank David Liversage for his interest, which opened for us an opportunity to plan a systematic examination of Danish Bronze Age objects, and Birthe Gottlieb and Marianne Lundbæk, who co-operated in the examination of the lurs. Part of this work was supported by a grant from Julie Damm's Studiefond, for which we are grateful.

Manuscript received 3. October 1989.

REFERENCES

ANER, E. & KERSTEN, K. 1973–88: *Die Funde der älteren Bronzezeit des nordischen Kreises in Dänemark, Schleswig-Holstein und Niedersachsen.* Band I–VIII Copenhagen-Neumünster.

BLAU, P.J. & LAWN, B.R. (editors) 1985: *Microindentation techniques in materials science and engineering.* ASTM, STP No. 889.

BÖHNE, C. 1965: Zur Frage der Härtung von Kupferwaffen und Geräte. *Technische Beiträge zur Zentralmuseum,* Mainz, p. 126–130.

BROHOLM, H.C. 1962: Et lurfund fra Hallenslev Mose, Vestsjælland. *Aarbøger for Nordisk Oldkyndighed og Historie* 1961: 147–159.

BROHOLM, H.C., SKJERNE, G. & LARSEN, W.P. 1949: *The lurs of the Bronze Age.* Copenhagen.

BRØNDSTED, J. 1939: *Danmarks Oldtid. II. Bronzealderen.* København.

CHARLES, J.A. 1985: Determinative mineralogy and the origins of mineralogy. *In British Museum Occasional Paper* No. 48:21–28.

COGHLAN, H.H. 1967: A metallurgical examination of eleven palstaves (from England and Ireland). *Journal of the Historical Metallurgy Society* 1:7–21.

DIES, K. 1967: *Kupfer und Kupferlegierungen in der Technik.* Springer-Verlag, Berlin.

GOLDSTEIN, J.I., NEWBURY, D.E., ECHLIN, P., JOY, D.C., FIORI, C. & LIFSHIN, E. 1984: *Scanning electron microscopy and X-ray microanalysis.* Plenum Press. New York 2nd Edition.

GOTTLIEB, B.A. 1987: X-ray analysis of a lur fragment. pp. 187–195 in *Publications issued by the Royal Swedish Academy of Music,* No. 53, editor C.S. LUND. Stockholm.

HANSON, D. & MARRYAT, C.B. 1927: Investigation of the effects of impurities on copper. Part III. The effect of arsenic. *Journal of the Institute of Metals,* 37:121–168.

HANSON, D. & PELL-WALPOLE, W.T. 1951: *Chill-cast bronzes.* London.

HAUPTMANN, A. 1985: 5000 Jahre Kupfer in Oman. Band 1: Die Entwicklung der Kupfermetallurgie vom 3. Jahrtausend bis zur Neuzeit. *Veröffentlichungen aus dem Deutschen Bergbau-Museum Bochum,* Nr. 33:136 pp.

HOLMES, P. 1986: The Scandinavian Bronze Lurs, pp. 51–125, in *Publications issued by the Royal Swedish Academy of Music,* No. 53, editor C.S. LUND, Stockholm.

JOVANOVIC, B. 1980: The Origins of copper mining in Europe. *Scientific American,* May: 114–120.

JUNGHANS, S., SANGMEISTER, E. & SCHRÖDER, M. 1960: *Metallanalysen kupferzeitlicher und frühbronzezeitlicher Bodenfunde aus Europa.* Berlin.

JUNGHANS, S., SANGMEISTER, E. & SCHRÖDER, M. 1968: *Kupfer und Bronze in der frühen Metallzeit Europas. Stand nach 12000 Analysen.* Berlin.

LA NIECE, S. & CARRADICE, I. 1989: White copper: The arsenical coinage of the Libyan revolt 241–238 B.C. *Journal of the Historical Metallurgy Society* 23:9–15.

LIVERSAGE, D. 1989. "Early Copper and Bronze in Denmark - a computer-aided examination of the SAM analyses", in J. POULSEN (ed.) *Regionale forhold i nordisk bronzealder.* Århus. Jysk Arkæologisk Selskabs Skrifter 24:47–60.

LIVERSAGE, D. & LIVERSAGE, M. 1989: A method for the study of the composition of early copper and bronze artifacts. An example from Denmark. *Helinium,* 29:42–76.

LYSDAHL, P. 1988: Lurerne fra Ulvkær. *Arkæologiske Udgravninger i Danmark* 1988, nr. 161, p. 129. Det Arkæologiske Nævn, København.

LYSDAHL, P. 1989: Fanfare. (Luren fra Ulvkær). *Skalk,* nr. 4:3–7.

MADDIN, R., WHEELER, T.S. & MUHLY, J.D. 1980: Distinguishing artifacts made of native copper. *Journal of Archaeological Science,* 7:211–225.

MAES, R. & DE STRYCKER, R. 1966: The copper-tin-arsenic constitution diagram. *Transactions of the Metallurgical Society of AIME,* 236:1328–1341.

MARÉCHAL, J.R. 1958: Étude sur le propriétés mécaniques des cuivres à l'arsenic. *Métaux.* 33:377–383.

MATTEOLI, L. & STORTI, C. 1982: Metallographic research on four pure copper flat axes and one related metallic block from an Eneolithic Italian cave. *Journal of the Historical Metallurgy Society 16*:65–69.

MCKERRELL, H. 1978 in A.D. FRANKLIN, J.S. OLIN & T.A. WERTIME (ed.) *The Search for Ancient Tin. U.S. Government Printing Office.* Wasington, D.C.

MCKERRELL, H. & TYLECOTE, R.F. 1972: The working of copper-arsenic alloys in the Early Bronze Age and the effect on the determination of provenance. *Proceedings of the Prehistoric Society* 38, 209–218.

METALS HANDBOOK 1973: *Metallography, structures and phase diagrams.* Vol. 8, 8th edition. American Society for Metals. Metals Park, Ohio.

MOESTA, H., SCHNAU-ROTH, G. & WAGNER, H.G. 1984: Mössbauer-Studien zu bronzezeitlichen Kupferhütten-Processen. *Berliner Beiträge zur Archäometrie,* 9:95–112.

MOOSLEITNER, F. & MOESTA, H. 1988: Vier Spangenbarrendepots aus Obereching, Land Salzburg. *Germania* 66:29–67.

NORTHOVER, J.P. 1982: The exploration of the long-distance movement of bronze in Bronze and Early Iron Age Europe. *Bulletin of the Institute of Archaeology* 19:45–72. London 1983.

OLDEBERG, A. 1974: *Die ältere Metallzeit in Schweden.* Vol. 1–2. Kungl. Vitterhets Historie och Antikvitets Akademien. Stockholm.

PARKER, G. 1982: Metallurgical notes on three Bronze Age implements found in the West of England. *Journal of the Historical Metallurgy Society* 16:46–49.

PERCY, J. 1861: *Metallurgy.* Vol. 1, Part 2: Copper, Zinc, Brass. Reprinted by De Archaeologische Pers Nederland, Eindhoven 1988.

RAMDOHR, P. & STRUNZ, H. 1967: *Lehrbuch der Mineralogie.* Stuttgart. 15. Auflage von Klockmann's Lehrbuch.

RIEDERER, J. 1987: *Archäologie und Chemie, Einblicke in die Vergangenheit.* Staatliche Museen, Rathgen-Forschungslabor. Berlin.

ROTHENBERG, B. 1980: Ingots from wrecked ship may help to solve ancient mystery. *Institute for Archaeo-Metallurgical Studies, Newsletter* No. 1, 2–3.

RYCHNER, V. 1984: La matière première des bronziers lacustres. *Archaeologie Suisse* 7:73–78.

SAVORY, H.N. 1980: *Guide catalogue to the Bronze Age Collection.* National Museum of Wales. Cardiff.

SCHULZ, H.D. 1984: Zuordnung von Kupfer-Metall zum Ausgangserz. *Praehistorische Zeitschrift* 58:1–14.

STRUNZ, H. 1970: *Mineralogische Tabellen*. Leipzig. 5. neubearbeitete Auflage.

TYLECOTE, R.F. 1976: *A history of metallurgy*. The Metals Society. London.

TYLECOTE, R.F. 1978 in A.D. FRANKLIN, J.S. OLIN & T.A. WERTIME (ed.) *The Search for Ancient Tin*. U.S. Government Printing Office. Wasington, D.C.

TYLECOTE, R.F. 1979: The effect of soil conditions on the long-term corrosion of buried tin-bronzes and copper. *Journal of Archaeological Science* 6:345–368.

TYLECOTE, R.F. 1980: Summary of results of experimental work on early copper smelting. *In British Museum Occasional Paper* No. 17:5–12.

TYLECOTE, R.F., BALMUTH, M.S. & MASSOLI-NOVELLI, R. 1983: Copper and bronze metallurgy in Sardinia. *Journal of the Historical Metallurgy Society* 17:63–78.

VANDKILDE, H. 1989: Det ældste metalmiljø i Danmark, in J. POULSEN (ed.) *Regionale Forhold i Nordisk Bronzealder*. Jysk Arkæologisk Selskabs Skrifter 24:29–45.

WILKINS, R.A. & BUNN, E.S. 1943: *Copper and copper base alloys*. McGraw Hill. New York.

YENER, K.A. & ÖZBAL, H. 1987: Tin in the Turkish Taurus mountains: the Bolkardag mining district. *Antiquity* 61:220–226.

YENER, K.A., ÖZBAL, H., KAPTAN, E., PEHLIVAN, A.N. & GOODWAY, M. 1989: Kestel: An early bronze age source of tin ore in the Taurus Mountains, Turkey. *Science* 244:200–203.